Front. Chem. Sci. Eng. 2023, 17(9): 1141–1161
https://doi.org/10.1007/s11705-022-2230-7

REVIEW ARTICLE

A review on co-pyrolysis of agriculture biomass and disposable medical face mask waste for green fuel production: recent advances and thermo-kinetic models

Melvin X. J. Wee[1], **Bridgid L. F. Chin** (✉)[1,2], **Agus Saptoro**[1], **Chung L. Yiin**[3,4], **Jiuan J. Chew**[5], **Jaka Sunarso**[5], **Suzana Yusup**[6], **Abhishek Sharma**[7,8]

1 Department of Chemical and Energy Engineering, Faculty of Engineering and Science,
Curtin University Malaysia, CDT 250, Miri 98009, Malaysia
2 Energy and Environment Research Cluster, Faculty of Engineering and Science, Curtin University Malaysia, CDT 250, Miri 98009, Malaysia
3 Department of Chemical Engineering and Energy Sustainability, Faculty of Engineering, Universiti Malaysia Sarawak (UNIMAS),
Kota Samarahan 94300, Malaysia
4 Institute of Sustainable and Renewable Energy (ISuRE), Universiti Malaysia Sarawak (UNIMAS), Kota Samarahan 94300, Malaysia
5 Research Centre for Sustainable Technologies, Faculty of Engineering, Computing and Science, Swinburne University of Technology,
Kuching 93350, Malaysia
6 Generation Unit (Fuel Technology & Combustion), Tenaga Nasional Berhad (TNB) Research Sdn Bhd, Kajang 43000, Malaysia
7 Department of Chemical Engineering, Manipal University Jaipur, Jaipur 303007, India
8 Chemical & Environmental Engineering, School of Engineering, RMIT University, Melbourne, Victoria 3000, Australia

Abstract The Association of Southeast Asian Nations is blessed with agricultural resources, and with the growing population, it will continue to prosper, which follows the abundance of agricultural biomass. Lignocellulosic biomass attracted researchers' interest in extracting bio-oil from these wastes. However, the resulting bio-oil has low heating values and undesirable physical properties. Hence, co-pyrolysis with plastic or polymer wastes is adopted to improve the yield and quality of the bio-oil. Furthermore, with the spread of the novel coronavirus, the surge of single-use plastic waste such as disposable medical face mask, can potentially set back the previous plastic waste reduction measures. Therefore, studies of existing technologies and techniques are referred in exploring the potential of disposable medical face mask waste as a candidate for co-pyrolysis with biomass. Process parameters, utilisation of catalysts and technologies are key factors in improving and optimising the process to achieve commercial standard of liquid fuel. Catalytic co-pyrolysis involves a series of complex mechanisms, which cannot be explained using simple iso-conversional models. Hence, advanced conversional models are introduced, followed by the evolutionary models and predictive models, which can solve the non-linear catalytic co-pyrolysis reaction kinetics. The outlook and challenges for the topic are discussed in detail.

Keywords biomass, COVID-19 waste, catalyst, pyrolysis, kinetics

1 Background

1.1 Bioenergy from biomass as a crucial renewable energy source

Association of Southeast Asian Nation (ASEAN) projected its population to grow by 100 million from 2014 to 2025, with an annual growth of 5%, and 4% in energy demand per year. Hence, the association has set the goal to increase its renewable energy share from 9.4% to 23% of the primary energy supply in the ASEAN region [1]. In order to meet the target, member countries has strategise several policies, laws, and regulations [2], as summarised in Table 1, which includes ASEAN member countries and their strategies [3].

Following this, ASEAN countries are known as the top agriculture producers. Hence, there are significant prospects for bioenergy as a strategy to help realise the ASEAN renewable energy generation and consumption goals. For example, Indonesia and Malaysia are the major players in the oil palm industry, followed by Thailand as

---

Received April 16, 2022; accepted August 8, 2022

E-mails: bridgidchin@curtin.edu.my, bridgidchin@gmail.com

Table 1 ASEAN member countries renewable energy policies

Country	Policies/strategies	Ref.
Cambodia	**Energy Sector Development Policy and Rural Electrification Policy, 2007** Rural electrification fund subsidy and investment incentives are provided as support to the policy • Providing reliable, affordable quality supply of electricity to the consumers • Promoting private-owned facilities in the renewable energy sector to instigate competition between the companies • Providing electricity to 70% of the rural households by the year 2030	[4]
India	**The Electricity Act, 2003** • To encourage the co-generation of electricity with renewable sources • Specify the terms and conditions for the determination of tariff, which forms the National Electricity Policy and the Tariff policy **Tariff Policy, 2006** • States that renewable energy shall be distributed with a preferential tariff determined by the appropriate commission • Bidding process within suppliers offering renewable energy from the same source **National Rural Electrification Policies, 2006** • Provision of access of electricity to all households by the year 2009 • Quality and reliable power supply at affordable rates • Providing off grid solutions for rural areas **Integrated Energy Policy Report (Planning Commission), 2006** Recommends a solution to meet the energy demand of India in an integrated process up to 2031–2032	[5]
Indonesia	**Government Rule No. 3 on Supply of Electricity, 2005** To ease the private-own power producers to set up renewable energy plants **Blueprint of National Energy Implementation Program 2005–2025** • To outline plans for energy supply security • To provide guidelines for various sectors involving renewable and non-renewable energies • To provide subsidies to enhance energy efficiency **Presidential Regulation No. 5 on National Energy Policy, 2006** • To set goals to promote diversification of energy sources • To reduce energy consumption by 1% per year as target **Presidential Decree No. 1 on Supply and Use of Biofuels, 2006** Setting targets and guidelines for biofuels utilisation and development **Ministerial Regulation No. 2 on Medium Scale Power Generation from Renewable Energy Sources, 2006** To set pricing guidelines for projects ranging from 1 to 10 MW **Energy Law, 2007** Providing renewable energy developers with investment incentives **Electricity Law, 2010** To encourage private companies to participate in energy supply To provide priority in the utilisation of renewable energy To promote small scaled distributed power generation from renewable sources **Ministerial Regulation No. 4/2012, 2012** To set the Feed-in-Tariff for electricity generated from biomass **Ministerial Regulation No. 27/2014, 2014** • To set goals to increase the renewable energy portion to 23% by the year 2025, and 31% by 2050 • Feed-in-tariffs for renewable energy • To encourage the government and private sectors to utilise biofuels for power generation	[6]
Malaysia	**Five-Fuel Diversification Policy, 2001** To include renewable energy in the energy supply mix of power generation **National Biofuel Policy, 2006** • To reduce dependency on fossil fuels • Providing subsidies to promote the demand for alternate sources of energy **National Renewable Energy Policy and Action Plan, 2010** • Increase the renewable energy contribution in the energy supply mix • Promote growth of the renewable energy sector • Maintaining the renewable energy at an affordable price • Instigate awareness to the community on renewable energy	[7]
Thailand	**Committee on Biofuel Development and Promotion (CBDP), 2008** Government subsidies from the State Oil Fund biodiesel price reduction **Second Alternative Energy Development Plan (2008–2022), 2008** • To increase the proportion of alternative energy to 20% of the national total energy consumption by 2022 • To utilise renewable energy as a substitute for imported oil • To increase energy security of Thailand • Promote integrated green energy utilisation in communities • Enhance the development of alternative energy industry • Research and development of efficient technology to harvest renewable energy	[8]
Vietnam	**Renewable Energy Action Plan, 2001** Government intervention to promote renewable energy **The Law of Electric, 2004** Support electricity generation from renewable sources by providing investment incentives, preferential electricity prices and taxes **Decision 1855/QD-TTg: 27 Dec 2007** • National Energy Development Strategy up to 2020 with outlook to 2050 • To encourage the development of new and renewable energies, bioenergy to meet the socioeconomic requirements • To meet the target of 5% of primary commercial energy by 2020 and 11% by 2050 **Decision No. 177/QD-TTg:20 Nov 2007** • To develop biofuel, as an alternative for fossil fuels • To build a legal framework for biofuel development • To develop materials for biofuel production • To enhance biofuel extraction **National Program for Biofuels Development, 2011** • Develop biofuel to partly replace fossil fuels • Create the legal framework for biofuel development • Develop relevant materials for biofuel production • Develop biofuel extraction technologies	[9]

(*Continued*)

Country	Policies/strategies	Ref.
Myanmar	**Myanmar Energy Master Plan, 2015** • To study the energy demand development from 2014 to 2035 • To set a goal to achieve 15%–20% share of renewable energy in 2020 • To improve the rural renewable energy usage • To achieve 57% hydropower, 5% solar and wind by 2030	[10]
Laos	**The Electric Law, 1997** Setting standards for the administration, production, distribution, transmission and the import and export of electricity **The Power Sector Policy Statement, 2001** • To increase the electricity supply rate to 90% by 2020 • Promotes the public and private partnerships in hydropower development (500 kV grid) **The 8th National Socio-economic Development Plan (NSEDP), 2016–2020** Promotes sustainability and diversification of renewable energy sources **The Renewable Energy Development Strategy** To increase the renewable energy share to 30% and substitute 10% of the transport fuel with biofuels by 2025	[11]
Philippines	**R. A. No. 9367: The Biofuels Act, 2006** Encourage the utilisation of biofuel-blended transport fuels by providing fiscal incentives **R. A. No. 9513: The Renewable Energy Act, 2008** • Enhance the renewable energy development by providing fiscal and non-fiscal incentives • To reduce the country's reliance of fossil fuels • Adopts renewable portfolio standards, feed-in-tariffs, net-metering, and Green Energy Option policy instruments	[12]

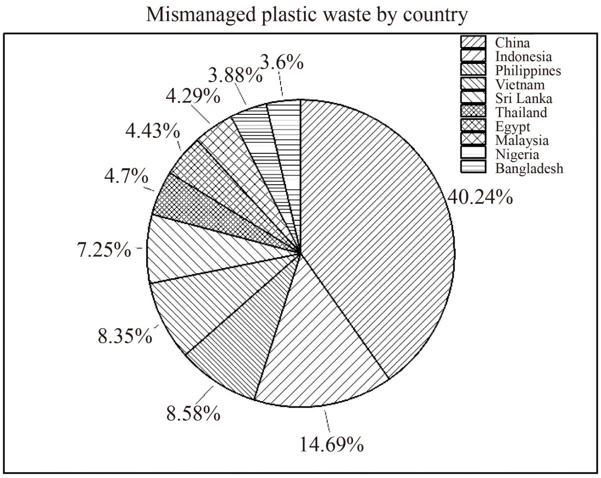

Fig. 1 Mismanaged plastic waste generated by countries. Reprinted with permission from Ref. [24], copyright 2015, American Association for the Advancement of Science.

shown in Fig. 1. In Indonesia, the production volume reached 45.86 million tonnes in 2019 [13]. Meanwhile, Malaysia produced 18.5 million tonnes in the same year [14]. However, the palm oil produced only represents 10% by weight of the total harvest; and the remainder contributed to the oil palm biomass, i.e., oil palm empty fruit bunch (EFB), palm kernel shell (PKS), palm pressed fibres (PPF), and oil palm frond [15]. To accommodate the rising population, food demand such as rice and wheat production in India has grown dramatically. In 1960, rice and wheat production was 34.6 and 11 million tonnes, respectively, and had risen to 118.9 and 107.6 million tonnes respectively in 2019 [16]. The rapid generation of biomass poses sustainability issues and waste management complications. Fortunately, this agriculture biomass is made up of lignocellulosic constituents, which include cellulose (23.3–44.9 wt %), hemicellulose (17.3–34.0 wt %), and lignin (12–53.5 wt %) [17]. Cellulose is a complex polymer of glucose held by β-1,4-glycosidic bonds, intramolecular and intermolecular H-bonds. Hemicellulose is a heterogeneous polysaccharide, consisting of hexoses (i.e., glucose, mannose, galactose, xylose, arabinopyranose, arabinofuranose, and glucuronic acid). Lignin is made up of guaiacyl propane, syringyl propane and *p*-hydrophenyl propane [17,18]. These constituents serve as the basic precursors for the conversion into fuel, fibres, and aromatics [19]. Other properties from the proximate and ultimate analysis are depicted in Table 2, which shows that the biomass contains 50 to 70 wt % of volatile matter. In comparison, the carbon and hydrogen contents are 36–53 and 5.0–7.3 wt %, respectively.

Besides that, plastic or polymer waste generation has increased over the years. According to Geyer et al. [23], the study reports that cumulative plastic waste generation of primary and secondary plastic has reached 6300 million tonnes from 1980 to 2015. Only 12% of these plastic wastes were incinerated, while 9% were recycled. Furthermore, according to Jambeck et al. [24], ASEAN member countries such as Indonesia, Philippines, Vietnam, Thailand, and Malaysia contributed approximately 41% of the mismanaged plastic waste as illustrated in Fig. 1. Moreover, according to Abnisa and Alaba [25], the global composition of plastic wastes comprises of 26.67% low density polyethylene (LDPE), 25.33% polypropylene (PP), 18.67% high density polyethylene (HDPE), 14.67% polyethylene terephthalate (PET), 8% polystyrene (PS), and 6.67% polyvinyl chloride (PVC). Furthermore, with the rapid rise of confirmed cases of the novel coronavirus disease (COVID-19), the need for personal protective equipment (PPE) is high, resulting in the rapid generation of COVID-19 related wastes, exacerbating the current plastic waste management issue. According to Liang et al. [26], there are two categories of COVID-19 related wastes which are (1) wastes generated

Table 2 Proximate and ultimate analysis of different agriculture biomasses [20–22]

Sample	PKS	PPF	EFB	Rice husk	Rice straw (RS)	Bagasse
Proximate analysis/(wt %)						
Moisture	5.73	6.56	8.75	4.50	–	–
Ash	2.21	5.33	3.02	12.40	13.60	6.50
Volatile matter	73.74	75.99	79.67	58.60	70.10	72.70
Fixed carbon	18.37	12.39	8.65	24.40	16.30	20.80
Ultimate analysis/(wt %)						
C	53.78	50.27	48.79	43.20	37.10	36.30
H	7.20	7.07	7.33	5.00	5.20	5.80
S	0.51	0.63	0.68	0.00	0.10	0.00
N	0.00	0.42	0.00	0.30	0.50	0.30
O	36.3	36.28	40.18	51.4	43.5	51.10

from within hospitals or healthcare facilities, which are considered medical wastes and are collected and disposed of with appropriate measures (i.e., identification, collection, separation, storage, transportation, treatment, and disposal) [26], and (2) the wastes generated outside those facilities, which include disposable medical face masks (DMFM) and gloves. These wastes do not have proper waste management and are often treated as municipal solid, and plastics wastes. Besides that, according to the World Health Organisation (WHO) [27], the demand for these PPE, i.e., DMFM, and gloves, is expected to rise 20% by the year 2025. If these wastes are not managed properly, it will lead to major environmental complications. In some parts of the ASEAN region (i.e., Cambodia, Philippines, India, and Indonesia), poor waste management issues such as landfills and illegal dumping were present even before COVID-19. These uncontrollable landfills would escalate into space limitations and release toxic pollutants to the environment [28]. Moreover, the random disposal of these wastes could also lead to microplastic pollution, accumulating in the food chain, especially in aquatic life [29].

1.2 Biomass and polymer waste conversion pathways: pyrolysis

Therefore, strategies to recover energy from these wastes are keys to minimize the waste accumulation and their impacts to the environment. To convert these high-energy feedstocks into valuable fuel, there are two main pathways to convert the lignocellulosic biomass and plastic wastes into biofuels or green fuels, i.e., bio-chemical conversion and thermochemical conversion. In bio-chemical conversion, the larger and complex compounds are broken down into simpler molecules, with bacteria and enzymes. However, this method has limited feedstock options, and is not suitable to convert synthetic polymers like plastic wastes [30]. Besides that, thermochemical conversion includes low-temperature carbonisation, intermediate-temperature pyrolysis, and high-temperature gasification. Among these thermochemical processes, pyrolysis represents a promising technology in terms of high fuel-to-feed ratios [31]. In addition, the pyrolysis process is favoured as the process that can be carried out at atmospheric pressure and faster conversion rates (<1 s) [32]. Moreover, the pyrolysis process is compatible with a wide variety of feedstocks aside from lignocellulosic biomass, i.e., plastics, and waste tires [33–36]. The pyrolysis process involves-production of biofuel in the form of bio-oil, as well as producing valuable bio-chemicals such as alcohols, aldehydes, ketones, acids, furans, anhydrosugars, and phenols from biomass [37]. Fast pyrolysis yields the highest amount of bio-oil (65–75 wt %), while slow pyrolysis produces less bio-oil (20–50 wt %), with a larger proportion of bio-gas (20–50 wt %) and biochar (25–35 wt %) [38]. A detailed information on the different pyrolysis modes can be found in these references [38–43].

This paper focuses on the issues of the growing generation of biomass in ASEAN region, as well as the single-use plastics (i.e., DMFM) generated due to the COVID-19 pandemic. Following this, this review outlines the potential of co-pyrolysis of the biomass with plastic wastes as a technique to produce value-added bio-oil. Besides that, this review also looks into the technologies, (i.e., catalyst selection) and technical aspects (i.e., pyrolysis parameters) of the co-pyrolysis process. In addition, the kinetic models, and the advancements to describe the catalytic co-pyrolysis of biomass and plastic wastes are also outlined. Finally, the outlook detailing the significance and the limitations of the co-pyrolysis technique is discussed.

2 Bibliometric analysis

Bibliometric analysis is defined as the analysis of scientific publications using statistical methods to provide an outline of the research area [44]. Several publications have adopted this method in research areas of bio-diesels [45], municipal solid waste management [44], investments [46], and even COVID-19 [47]. This method of analysis provides a systematic way to sort and analyse a great number of publications, in terms of citations, co-citations, author keywords, and countries.

In this project, the bibliometric analysis of the field of pyrolysis of biomass was conducted in VOSviewer1.6.11. The utilisation of the software has been widely employed in this study, providing a visualisation of the relationships between publications in a research area or topic. The online publication database platform, Scopus, was utilised in the collection of the database for this study. The search phrase and Boolean Operators for this study were “pyrolysis AND biomass AND plastic AND bio-oil OR oil palm OR catalyst”, the publication year was limited from 2019 to 2023, and limited to journal articles only. A total of 1448 publications were fitted into VOSviewer to analyse the co-occurrence of author keywords more than 20 times and are visualised in Fig. 2. The top-ranked link strength keywords, excluding the search phrases, include catalytic pyrolysis, co-pyrolysis, biochar, oxygen reduction reaction, and hydrogen. Based on this study, the current research trend involves around catalytic pyrolysis or co-pyrolysis, and focuses on the oxygen reduction, hydrogen and biochar formation from the process. Furthermore, another analysis of the bibliographic coupling of countries was carried out and the results were visualised in Fig. 3. The result suggests that China, United States, South Korea, Malaysia, and Australia are the active countries involved in this research area.

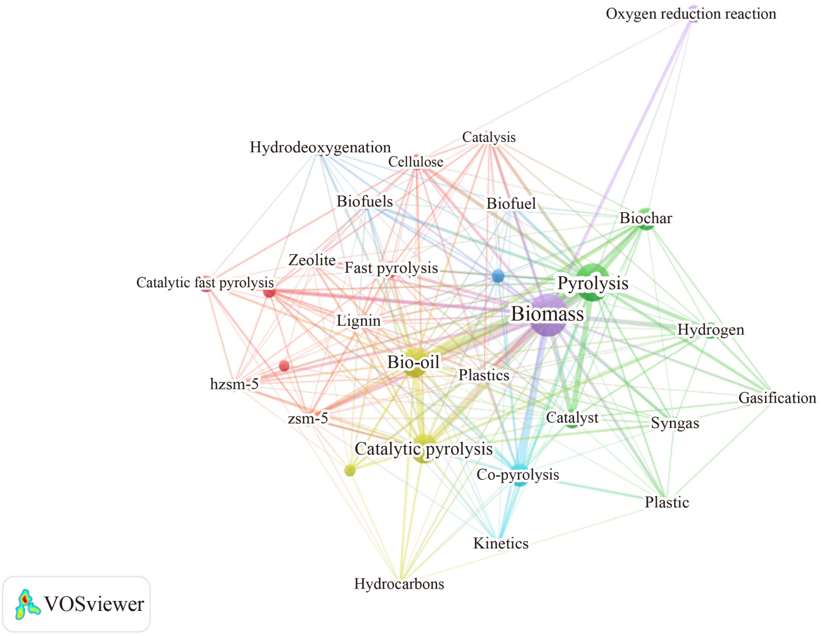

Fig. 2 Co-occurrence of author’s keywords > 20 times by publication year.

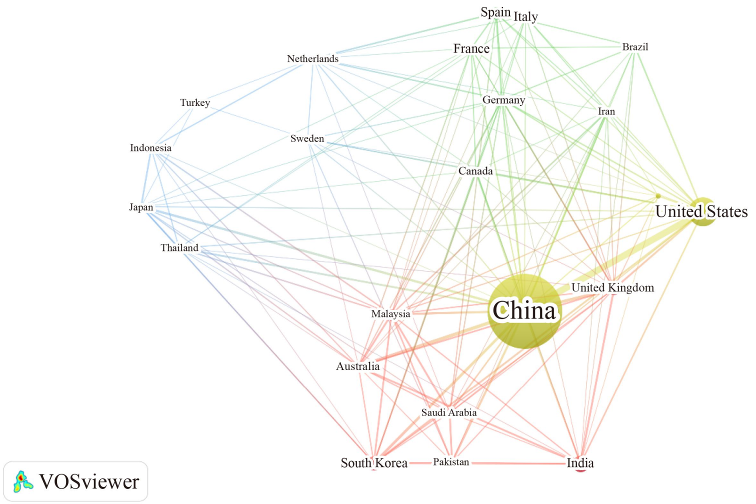

Fig. 3 Bibliographic coupling of countries by year.

3 Pyrolysis technologies/techniques for bio-oil production

Initially, most of the research studies focus on mono-component such as biomass [20,48–54] or plastic waste [55–60] in the pyrolysis process for bio-oil production. However, the pyrolysis of lignocellulosic biomass produces low quality bio-oil and yield [61]. Biomass-derived pyrolysis oil is high in oxygen content, corrosive in nature, and thermally unstable. Bio-oil generally requires upgradation using a hydrogen source and a catalyst, which makes the process complicated and expensive [37]. For plastic pyrolysis, the volatile products contain harmful compounds, i.e., polycyclic aromatic hydrocarbons (PAHs) [62–64]. PAH is a macromolecular aromatic compound with carcinogenic and mutagenic characteristics that pose health concerns upon exposure [65]. Hence, there is a growing interest in improving the pyrolysis process to produce bio-oil with enhanced properties, i.e., co-pyrolysis of two or more feedstock, and the utilisation of catalysts for product upgrading.

3.1 Mechanisms of co-pyrolysis with polymers

Hence, it is crucial to understand the reaction mechanism of co-pyrolysis of biomass and plastic wastes. Several studies have explored the co-pyrolysis of biomass with polymer wastes, i.e., RS and sugarcane bagasse with PP, and PS [34]; corn stover, ipil, and narra, with HDPE, LDPE and PP [35]; RS with waste tires [36]; sawdust with LDPE [66]. These studies show that the co-pyrolysis technique is promising in improving the bio-oil quality and calorific value, reducing energy costs by lowering the activation energy. According to Lin et al. [67], the widely accepted mechanism of co-pyrolysis of biomass with plastics can be summarised in a two-step mechanism: (1) the free radicals generated from the pyrolysis of biomass initiate the β-scission of the polymers, inhibiting the intermolecular and intramolecular H transfer, producing aliphatic hydrocarbons and reduced alkadienes; (2) the H transfers from the polymers reacting with the biomass-derived radicals to form stable compounds. This mechanism allows an increase in the decomposition rate of the biomass, greatly reducing the char yield as reported by Önal et al. [68]. The addition of a hydrogen-rich plastic waste to biomass influenced the energy recovery efficiency of bio-oil by affecting the real-time power output, reaction time, and changes in the bio-oil composition [69]. Besides that, the biomass decomposes first at a lower temperature forming free radicals, i.e., OH radicals. These radicals react with the pyrolysis products of plastic, larger molecular weight organics (C_{12}) were formed with the co-pyrolysis of biomass and LDPE [70]. According to Navarro et al. [34], this mechanism reduces the selectivity for the secondary reaction to occur, reducing the char yield (i.e., 8.6 and 10 wt % reduction of char with the co-pyrolysis of B and PS, B and PP, respectively). Besides that, according to a study by Ojha et al. [71], the formation of C_8–C_{20} alcohols was observed, which was explained by the reaction of hydrocarbon free radicals from PP, with water from the dehydration reaction from cellulose. According to Uzoejinwa et al. [72], synthetic polymers are derived from petroleum products with high carbon and hydrogen contents, low oxygen content, and contains high calorific values. Hence, making it suitable potential as a co-feedstock for the biomass pyrolysis. Furthermore, these polymer wastes also showed similar properties of high volatile matter, higher heating value (HHV) and lower heating value (LHV) than biomass, as observed in Table 3.

3.2 Pyrolysis reaction parameters that influence the bio-oil yield

During pyrolysis, multiple factors affect the outcome of the process, which are, reactor temperature, heating rate, feedstock particle size, and residence time. Studies on these parameters are crucial to improve the pyrolysis process in terms of bio-oil product yield and quality. Generally, the operating parameters are adjusted, to impede the secondary tar cracking reactions, which reduces the bio-oil yield.

3.2.1 Pyrolysis temperature

The role of temperature is to provide sufficient thermal energy for the decomposition of the biomass. It is important to note that for the main constituents of biomass, cellulose, hemicellulose, and lignin, their temperature degradation ranges are 225–325, 325–375, and 250–500 °C, respectively. Hence, an optimal temperature of 500 °C is sufficient to encompass these temperature ranges. Nevertheless, the optimal temperature differs with the compositions of varying feedstock [74]. Furthermore, according to Dai et al. [75], bio-oil yield peaks at the

Table 3 Proximate and ultimate analysis of polymers [22,34,60,73]

Sample	PP	PS	LDPE	HDPE	Waste tires
Proximate analysis/(wt %)					
Moisture	0.20	–	–	0.00	1.10
Ash	0.10	0.00	–	0.00	8.10
Volatile matter	99.80	99.50	99.98	100.00	62.50
Fixed carbon	0.00	0.50	0.02	0.00	28.20
Ultimate analysis/(wt %)					
C	85.40	89.50	85.47	85.34	84.60
H	14.50	8.50	14.21	12.22	7.70
S	0.00	0.00	0.11	0.00	1.40
N	0.00	0.00	0.08	0.00	0.40
O	0.00	2.00	0.13	2.44	4.30
HHV/(MJ·kg^{-1})	46.00	40.10	–	46.40	36.80
LHV/(MJ·kg^{-1})	43.10	–	–	43.10	35.10

temperature range of 450–550 °C; a further increase of temperature (> 600 °C), the bio-oil yield reduces, corresponding to an increase in non-condensable gas, or biogas. Moreover, a higher temperature (530–830 °C) promotes the reduction of complex compounds (i.e., acetaldehyde, methanol, propanol, and acetone), while increasing stable compounds (benzene, naphthalene, cresols, and phenols). For the case of polymer wastes, the degradation temperature ranges generally overlap or are higher than biomass, which varies between types of polymers. According to Miandad et al. [33], PP showed a single-stage degradation, which starts at a lower temperature of 240 °C with the maximum degradation at 425 °C, PS also showed a single-stage degradation but starts at a higher temperature of 330 °C, with the maximum degradation at 470 °C. While polyethylene (PE) exhibits a two-stage degradation, the first stage starts at the temperature of 270 °C and reaches 400 °C with a conversion rate of 12%, which followed by the second stage degradation starting at 400 °C, with the maximum conversion rate of 95% at 480 °C. Hence, these differences in thermal decomposition behaviours must be considered for the co-pyrolysis of biomass and polymers. According to Salvilla et al. [35], the study studied the effect of co-pyrolysis of corn stover with different polymers, i.e., LDPE, PP, and HDPE. Thermogravimetry analysis (TGA) experiments of the biomass-plastic blends result in a two-stage decomposition. The first stage involves the degradation of hemicellulose, and cellulose of the corn stover, while the second stage degradation overlaps with the decomposition of lignin. The results from this study conclude that the biomass and plastic blends exhibit the most synergistic effect occurs at temperature near 500 °C, i.e., corn stover and PP blend (5:3), and corn stover and LDPE blend (5:3) observed the greatest decomposition rate between 8% and 10% per minute respectively between the temperature ranges of 480–505 °C.

3.2.2 Heating rate

The heating rate is another important parameter that could determine the product distribution of the biofuels. According to Akhtar and Saidina Amin [31], fast heating rates cause rapid fragmentations of biomass and produces more bio-oil yield. This is possible as at higher heating rates (1000 °C·min^{-1}), there is short amount of time for the secondary reactions (i.e., tar cracking and repolymerisation). However, once the heat and mass transfer limitations have been overcome, higher heating rates would not increase the bio-oil yield further. Besides that, heating rates also affect the quality of the bio-oil, at lower heating rates, the water content of the bio-oil increases, as it impedes the dehydration reaction. It is also observed that at low heating rates (< 15 °C·min^{-1}) the bio-oil components have a higher weight range of 500–1000 Da, while increasing the heating rate to 15 °C·min^{-1}, it significantly reduces the weight to 200–500 Da. However, continuing to increase the heating rate does not reduce the weight further [75]. In the case of polymer waste, the study found that LDPE, PP, and PVC, the thermogravimetry or derivative thermogravimetry curves shifted to the higher temperatures when the heating rate was increased. This phenomenon was explained by the thermal lag, due to the increased thermal gradient between the furnace temperature and the sample. Hence, the lower 100 °C·min^{-1} heating rate favoured the degradation of the plastic wastes [60].

3.2.3 Particle size

To reduce heat transfer limitations caused by the poor heat conductivity of biomass, feedstock particle size or shape is another important criterion for bio-oil production. Larger particles (> 0.5 mm) tend to have poor heat transfer to the inner surfaces of the feedstock particle, this will lead to a lower yield of volatiles associated with the great temperature differences between the inner and outer surfaces of the feedstock particle. However, it is documented further increase in particle size (> 1 mm) does not have any effect on the bio-oil yield, which indicates minor impact of the internal heat or mass transfer to the process [76]. It was also reported that larger particle size, results in lower heat transfer to the feedstock [31,75]. For the pyrolysis of bamboo biomass with particle size, 0.45–0.75 mm, the bio-oil peaked at 54.03 wt %, while for smaller particle size 0.25–0.45 mm lowers the bio-oil yield to 50.85 wt % but increases biogas yield from 18.42 to 23.46 wt % [77]. Larger particle size of 0.8–1.2 mm, on the other hand, also lowered bio-oil yield of 51.61 wt %, with increased biogas and biochar yield of 20.62 and 27.74 wt %, respectively.

3.2.4 Residence time

Likewise, since the pyrolysis vapour is susceptible to secondary reactions, it is important to note that, the vapour residence time must be kept short to maximise the bio-oil yield. However, at very short residence times, the heat transfer limitations may restrict the feedstock from undergoing complete fragmentation [32,74,75]. Hence, the parameter is restricted by the characteristic of the feedstock itself. Instead, optimisation of the vapour residence time is a more feasible direction, i.e., feedstock particle size, heating rate, and design of the reactor and heater configuration to maximise the heat transfer [31].

3.3 The role of catalysts in the pyrolysis process

Catalysts play an important role in enhancing the quality of the bio-oil. This section categorised the existing catalysts employed in the pyrolysis process into three main groups, commercial zeolite catalysts, metal-based catalysts, and renewable waste catalysts.

3.3.1 Commercial zeolite or acid catalyst

The commercial zeolite catalysts, i.e., ZSM-5, HZSM-5, MCM-41, zeolite Y, SBA-15, and zeolite BEA are the commonly utilised catalysts for the pyrolysis of biomass [78]. These catalysts have the active sites of the catalysts and reduce the dissociation energy of C–O, C=O, and –OH functional group, which allow the ability to remove oxygen atoms from the bio-oil via dehydration, decarboxylation, decarbonylation reactions [42,79]. Besides that, according to Ratnasari et al. [80], the key attributes of the zeolite as a suitable catalyst are the micropores (0.4–1.0 nm) or mesopores (1.5–30 nm) sizes. In a study on MCM-41, a zeolite catalyst with a mesoporous structure; the bigger pores allow hydrocarbons with higher molecular weight to enter the active sites, produce less oxygenates, and yield less aromatics. While smaller pore sized zeolites, such as ZSM-5 and Y-zeolite favour the production of aromatics. However, due to its smaller pore size, it is more likely to cause coking on the surface of these zeolites, thereby deactivating them. Therefore, studies have incorporated hierarchical catalyst structure to maximise the conversion performance [78,81]. Besides that, the acidity of the zeolites refers to the Si/Al ratio of the zeolite, it is a direct representation of the Brønsted acid (–OH group) and Lewis acid (Al sources in the Al_2O_3/SiO_2) sites available [74]. Comparing with zeolites, the silicalite catalyst with the same pore size but without acidity produces less aromatics and increases char formation [32]. Besides that, a study on the catalytic co-pyrolysis of RS and B with plastic wastes concluded that HZSM-5 promoted the deoxygenation, cleavage of the aromatic rings, reforming, isomerisation and Diels−Alder reaction of the bio-oil [22]. Hence, product upgradation was achieved, and thereby producing valuable compounds, such as aromatics (i.e., styrene, ethylbenzene, *o*-xylene, and trimethyl-benzene) and aliphatic hydrocarbons (i.e., 2,4-dimethyl heptane). Zhao et al. [82] found that, with the bamboo to PP ratio of 1:2 over HZSM-5, high bio-oil yield of 61.62 wt % can be achieved, which is higher compared to that obtained for single feedstock bamboo pyrolysis of 29.91 wt %. Besides that, the aromatic and naphthenic hydrocarbons in the bio-oil were improved, which was in agreement with the study by Suriapparao et al. [22], where with the addition of a catalyst, the biomass−plastic mixture has a lower selectivity for oxygenates, while an increase in aliphatic and aromatic hydrocarbons were observed. The findings summarising the commercial acid catalysts utilised in literature can be found in Table 4.

3.3.2 Commercial metal-based catalyst/support

The metal-based catalysts in the catalytic pyrolysis of biomass majority refers to the metal oxides, alkali earth metals, metal salts, and transition metals. Metal oxides are prominent catalysts in this case, i.e., the basic MgO, CaO, and the acidic ZnO in the study of the pyrolysis of RS. The catalytic behaviour of MgO is similar to ZSM-5, as it favours the ketonization and aldol condensation reactions, which help to reduce oxygenates from the bio-oil [75]. According to Cao et al. [83], MgO has high ionic properties, which inhibits the repolymerisation reaction, hence greatly reduces the biochar formation while increasing the bio-oil yield. Furthermore, CaO was determined to have unique properties, as it behaves differently at different mass ratio incorporated in the feedstock, at less than 0.2 mass ratios; the CaO is a reactant, that reacts with the carboxyl groups to produce ketones. Carboxyl groups are undesirable bio-oil products due to their acidity, i.e., acetic acid. At 0.2 to 0.4 mass

Table 4 Acid zeolite catalyst application in the pyrolysis process examples

Biomass	Catalyst	Bio-oil yield/(wt %)	Reactor	Scale, feed weight/g	Ref.
RS	HZSM-5	21.50	Microwave pyrolysis	200–800	[22]
Bagasse		22.40			
PP		74.20			
PS		92.30			
Baggase: PS		43.80			
B:PP		35.70			
RS:PS		31.20			
RS:PP		24.50			
RS	ZSM-5	47.40	Fixed bed reactor	10	[83]
	Y zeolite	55.20			
	Mordenite	49.10			
	SBA-15	37.30			
Rice husk and WGPF	HZSM-5/MCM41	67.90% hydrocarbon relative content	Tubular reactor	0.001	[81]
	HZSM5	60.20% hydrocarbon relative content			
Seaweed biomass	ZSM-5	51.48	Hydro-pyrolysis	10	[32]
	MCM-41	41.84			
Bamboo	HZSM-5	49.14	Bubbling fluidised bed	100 g·h^{-1}	[77]

ratio, CaO exhibits absorbent properties, absorbing CO_2 to $CaCO_3$, which contributes to the mass increase in the char yield. A further increase of CaO (> 0.4 mass ratio), the catalytic effect dominates, reducing the ester content in the bio-oil into simpler hydrocarbons and H_2 [84]. Besides that, while ZnO has less deoxygenation properties compared to CaO and MgO, it does not increase biochar yield [32,75,85]. On the other hand, studies have also found that metal salts have effectively improved the bio-oil yield. In a study of metal salt catalysts, $MgCl_2$ produced the maximum bio-oil yield of 48.4 wt % [83], comparing to the transition metal salt $FeCl_3$, which has a lower bio-oil yield of 32.2 wt %. According to the study, the ionic behaviour of the alkali earth metal salt, $MgCl_2$ minimises the repolymerisation reaction compared to the partial covalent transition metal salts. In recent studies of the plastic pyrolysis process, the metal catalysts such as carbon-supported platinum (Pt/C), and palladium (Pd/C) were studied in the pyrolysis of PET plastic. The study aims to reduce the polycyclic compounds and biphenyls which are harmful compounds to the environment and public health. The study concludes that Pt/C aided in the reduction of polyclyclic compounds such as 2-napthalenecarboxylic acid by 102% at 800 °C, and reduction of biphenyls such as biphenyl-4-carboxylic acid by 27% at 700 °C [86]. Furthermore, metal oxides have been employed to study the co-pyrolysis process of PP with poplar wood (i.e., ZnO, CaO, MgO, and Fe_2O_3). The researchers found that CaO has the best deoxygenation results, removing carboxylic acids and phenols from the final products. It also increases cyclopentanones and alkenes compositions, but has reduced total volatile compounds, due to its strong basicity to cause coking on the catalyst surface. ZnO has the highest alkene yield, and increased ketone and phenols yields, and reduced carboxylic acid but has the weakest deoxygenation activities among all four catalysts. MgO behaves similarly to CaO, but has weaker deoxygenation properties, as it is less basic than CaO. Moreover, in the presence of the Fe_2O_3 catalyst, formation of aromatics such as *p*-xylene and 2-methyl-1-butenylbenzene were formed [87]. Following this, the studies of metal-based catalysts are summarised in Table 5, CaO is widely utilised in many studies due to its abundance and low cost, which can be found in renewable sources such as limestone and eggshells [88], and the niche in the utilisation of metal catalysts in the co-pyrolysis process.

3.3.3 Renewable waste catalyst

Renewable waste catalysts received much attention as an economic and sustainable alternative to commercial catalysts, i.e., red mud, ash catalysts, activated carbon, biochar derived catalyst, and palm oil sludge [90–94]. Red mud has attained much research interest as it has the potential to replace commercial catalyst. It is an alkaline

Table 5 Metal based catalyst application in the pyrolysis process examples

Biomass	Catalyst	Category	Bio-oil yield/(wt %)	Reactor	Scale, feed weight/g	Ref.
EFBF	CaO	Basic metal oxide	39.90 (5 wt % CaO); 40.40 (10 wt % CaO)	Fixed bed reactor	15	[85]
	MgO	Basic metal oxide	39.30 (5 wt % MgO); 42.30 (10 wt % MgO)			
	ZnO	Acidic metal oxide	44.70 (5 wt % ZnO); 42.20 (10 wt % ZnO)			
Cotton stalk	CaO	Basic metal oxide	50.00	Fixed bed reactor	–	[84]
RS	$MgCl_2$	Metal salt oxide	48.40	Fixed bed reactor	10	[83]
	$FeCl_3$	Metal salt	32.20			
	$CuCl_2$	Metal salt	41.50			
	$MnCl_2$	Metal salt	45.30			
	CaO	Basic metal oxide	38.70			
	$CaCO_3$	Basic metal oxide	30.50			
	MgO	Basic metal oxide	52.10			
	$MgCO_3$	Basic metal oxide	42.40			
	CeO_2	Acidic metal oxide	52.30			
	ZnO	Acidic metal oxide	46.20			
	ZrO_2	Acidic metal oxide	48.30			
	TiO_2	Acidic metal oxide	48.20			
EFB	CaO	Basic metal oxide	58.49	Fixed bed reactor	50	[89]
PET	Pt Pd	Metal catalyst	–	Tube furnace	1	[86]
PP-poplar wood composite	ZnO	Acidic metal oxide	–	Pyrolysis-gas chromatography/mass spectrometry	0.5 mg	[87]
	CaO	Basic metal oxide				
	Fe_2O_3	Acidic metal oxide				
	MgO	Basic metal oxide				

solid by-product from the Bayer process in alumina production. According to Ly et al. [77], the components within the red mud include a great amount of metal oxides, i.e., MgO, CaO, SiO_2, Fe_2O_3, Al_2O_3, and TiO_2. From the study, red mud has a comparable bio-oil yield than HZSM-5 at temperature of 475 °C and residence time of 1.8 s. Upon characterisation of the bio-oil produced from red mud, the catalyst promoted the depolymerisation of cellulose and hemicellulose to produce furan derivatives. Besides that, the formation of saturated phenols in the bio-oil indicates red mud favours the demethylation and demethoxylation reactions. Furthermore, researchers have also studied the catalytic effect of the pyrolysis biochar. According to Dong et al. [95], the experiment on the catalytic pyrolysis of bamboo waste with different ratios of biochar, concluded that, the bio-oil had been upgraded; simpler C_2–C_6 compounds have been greatly increased with reduction in the heavy C_7–C_{11} compounds. Moreover, Chen et al. [96] proposed upgrading the biochar from the pyrolysis process such as N-doped biochar, found high yields of bio-oil (61.0–63.0 wt %) were obtainable. A study on the Fe incorporated activated carbon reduces the bio-oil yield to achieve increased phenols 60.85–86.98 wt % of the bio-oil [97]. For the pyrolysis of plastic wastes, most research utilises the low-cost fly ash and naturally occurring kaolin as renewable catalyst sources [98–100]. Furthermore, in the case of co-pyrolysis, renewable waste catalysts such as Ni-doped biochar from waste pine sawdust, and activated carbon made from coconut husks were utilized [101,102]. The summary of renewable waste catalysts is depicted in Table 6, shows that renewable waste in the literature has much lower bio-oil yields or has a higher selectivity to syngas production than commercial catalysts.

4 Kinetic analysis

Kinetic analysis is an important aspect in describing the chemical kinetics of the pyrolysis process in the form of mathematical models. Traditionally modelling the chemical kinetics of biomass pyrolysis considers cellulose, hemicellulose, and lignin, based on the TGA experimental data. These kinetic models include the iso-conversional models, the Vyazovkin method, distributed activation energy model (DAEM), and the utilisation of predictive tools, i.e., artificial neural network (ANN).

4.1 Iso-conversional models

Iso-conversional method is the simplest form of kinetic model to explain the conversion of biomass to volatiles and biochar as a one-step first-order reaction. Examples of the iso-conversional method include the Kissinger–Akahira–Sunose (KAS), Flynn–Wall–Ozawa (FWO), and Starink's method, which are integral methods ($g(\alpha)$). In contrast, the Friedman method is an example of a differential method ($f(\alpha)$) [104]. In this paper, Friedman and Starink's methods are chosen to demonstrate the difference between the differential and integral versions of the iso-conversional method.

4.1.1 Friedman method

Friedman method is based on the differential method as the following expression in Eq. (1). This method requires the information on the conversion rate $\frac{\mathrm{d}\alpha}{\mathrm{d}t}$, and T. The kinetic plots between $\ln\left(\frac{\mathrm{d}\alpha}{\mathrm{d}t}\right)$ and $\frac{1}{T}$ produce the slope of

Table 6 Renewable waste catalyst for pyrolysis process examples

Biomass	Catalyst	Bio-oil yield/wt %	Reactor	Scale, feed weight/g	Ref.
Bamboo	Biochar	20.20 (5 wt % biochar) 18.70 (10 wt % biochar) 16.34 (20 wt % biochar)	Microwave pyrolysis	50	[95]
Bamboo	N-doped biochar	61.00 (10 wt % biochar) 63.00 (30 wt % biochar) 62.00 (50 wt % biochar)	Fixed bed reactor	3	[96]
PKS	Fe/activated carbon	7.96	Microwave pyrolysis	10	[97]
Rice husk	Rice hull ash	–	Fixed bed reactor	0.0055	[92]
Rice husk	Coal bottom ash	–	Fixed bed reactor	0.0055	[93]
PKS	Red mud	37.37–39.95	Fixed bed reactor	2	[103]
Bamboo	Red mud	50.34	Bubbling fluidised bed	100 $g\cdot h^{-1}$	[77]
EFB	Palm oil sludge	–	Fixed bed reactor	15	[90]
LDPE	Calcinated fly ash (900 °C)	76.22–80.02	Semi batch reactor	50	[98]
	Calcinated fly ash (800 °C)	70.96–71.36			
	Natural fly ash	68.20–71.70			
HDPE (plastic tub pieces)	Fly ash (10 wt %)	50.84	Lab scale pyrolyzer unit	1 kg	[100]
LDPE	Kaolin (1350 mesh)	64.66% aliphatics, 93.91% hydrocarbons, 30.07% H_2	Quartz furnace tube	100	[99]
Pine sawdust and PE (50 wt %)	Ni-pine sawdust biochar	70.40 wt % (gas yield)	Fixed bed reactor	1	[101]
Corn stalk-HDPE mixture	Activated carbon	–	Tubular reactor	2	[102]

$\frac{E}{R\cdot T}$ and the intercept of $\ln[Af(\alpha)^n]$. The benefit of this model is that it makes no approximations, and can be adopted in any temperature settings [105],

$$\ln\left(\frac{\mathrm{d}\alpha}{\mathrm{d}t}\right)=\ln[Af(\alpha)^n]-\frac{E}{R\cdot T},\tag{1}$$

where $f(\alpha)$, T, A, R, E are the differential form of the kinetic dependence function, absolute temperature (K), exponential factor (s^{-1}), universal gas constant (8.314 $\mathrm{J\cdot mol^{-1}\cdot K^{-1}}$), activation energy ($\mathrm{kJ\cdot mol^{-1}}$).

4.1.2 Starink's method

Starink's method is an extension of the Coats–Redfern equation (Eq. (2)), which is similar to the FWO method, an integral method for estimating kinetic parameters [105]. Since $2RT/E \leqslant 1$, and has minimal variation with T, results in Eq. (3),

$$\ln\left(\frac{\beta\cdot g(\alpha)}{T^2}\right)=\ln\left[\frac{A\cdot R}{E}\left(1-\frac{2R\cdot T}{E}\right)\right]-\frac{E}{R\cdot T},\tag{2}$$

$$\ln\left(\frac{\beta\cdot g(\alpha)}{T^2}\right)\cong\ln\left(\frac{A\cdot R}{E}\right)-\frac{E}{R\cdot T},\tag{3}$$

where β, $g(\alpha)$ are the heating rate ($\mathrm{°C\cdot min^{-1}}$), and the integral form of the kinetic dependence function. The generalised form Eq. (4) is

$$\ln\left(\frac{\beta\cdot g(\alpha)}{T^m}\right)=B-C\left(\frac{E}{R\cdot T}\right).\tag{4}$$

Starink's equation utilises the constants, where m = 1.92, $B = \ln(AR/E) + 3.7545411 - 1.92\ln E$, and C = 1.0008, which can be rewritten as Eq. (5),

$$\ln\left(\frac{\beta}{T^{1.92}}\right)=C_{\mathrm{s}}-1.0008\left(\frac{E}{R\cdot T}\right),\tag{5}$$

where C_{s} is the constant. This method is a simple direct method to obtain the expression E/R from the slopes by plotting $\ln\left(\frac{\beta}{T^{1.92}}\right)$ vs. $1/T$. Starink's method is widely employed as a comparison against other iso-conversional methods [48,106]. However, these methods are flawed, as proposed, with an addition of a secondary feedstock and the utilisation of a catalyst, the reaction mechanisms become much more complex [107]. Hence, a modified iso-conversional method is introduced, the Vyazovkin method.

4.2 Vyazovkin method

The iso-conversional methods assume a reaction ideally has a constant value of E_α. This assumption is the main source of errors, which explains the differences obtained from different iso-conversional methods [105]. Hence, to overcome these drawbacks, an advanced alternative non-linear iso-conversional Vyazovkin method is proposed. This method assumes the reaction is independent of the heating rate, and accounts for the variation of E in the computation of the temperature integral, $I(E_\alpha,T_\alpha)$ from Eq. (6). The E_α, which is the effective activation energy ($\mathrm{kJ\cdot mol^{-1}}$) is obtained from the minimisation of the function $\varnothing(E_\alpha)$ from Eq. (7),

$$I(E_\alpha,T_\alpha)=\int_0^{T_\alpha}\left(-\frac{E_\alpha}{R\cdot T}\right)\mathrm{d}T=\frac{E_\alpha}{R}p(x),\tag{6}$$

$$\varnothing(E_\alpha)=\sum\nolimits_i^n\sum\nolimits_{j=i}^n\left(\frac{I(E_\alpha,T_{\alpha,i})}{I\left(E_\alpha,T_{\alpha,j}\right)}\cdot\frac{\beta_j}{\beta_i}\right),\tag{7}$$

where n, E_α, T_α are the number of heating rates in the experiment, activation energy and temperature for each α, while i and j represent the heating rates corresponding to n. For $p(x)$, it is the approximation equation obtained from using Yang equation, Eq. (8):

$$p(x)=\frac{\exp(-x)}{x}\cdot\frac{x^3+18x^2+88x+96}{x^4+20x^3+120x^2+240x+120},\tag{8}$$

where x is the simplified expression of E/RT. Hence, due to its complex structure, this model requires a numerical approach to solve for the kinetic parameters. Recent studies have started adopting this method to compute the kinetic parameters [48,54].

4.3 Distributed activation energy model

In a complex process such as co-pyrolysis, the E_α would not be constant. Instead, it varies as an indication of a much more complex reaction in place, which is unable to explain over a single-step kinetic model. The DAEM is an accurate and versatile model to represent complex pyrolysis processes. It is the best mathematical method to show the physical and chemical heterogeneity of biomass during a devolatisation process [34]. According to Hameed et al. [107], DAEM takes into consideration of the decomposition of species over a large number of independent parallel reactions with different activation energies, represented by a continuous distribution function (i.e., Gaussian distribution, $f(E)$), Eq. (9):

$$f(E)=\frac{1}{\sigma\sqrt{2\pi}}\exp\left[-\frac{1}{2}\left(\frac{E-E_{\mathrm{M}}}{\sigma}\right)^2\right],\tag{9}$$

where σ, E_{M} are the standard deviation and the mean activation energy, respectively. Furthermore, studies have simplified the DAEM based on the assumption that the solid feedstock is a complex mixture of compounds. During the pyrolysis process, a great number of independent consecutive or simultaneous, irreversible reactions take place, each characterised by its corresponding activation energies and pre-exponential factor, given by Eq. (10):

$$1-\alpha=\int_0^\infty\exp\left(-A\int_0^t\exp\left(\frac{E}{RT}\right)\mathrm{d}t\right)\cdot f(E)\,\mathrm{d}E=\varnothing,\tag{10}$$

where, according to Cano–Pleite et al. [108], $\varnothing$ = 0.58, which can be simplified as Eq. (11):

$$\ln\left(\frac{\beta}{T}\right)=\ln\left(\frac{A\cdot R}{E}\right)+0.675-\frac{E}{R}\cdot\frac{1}{T}. \tag{11}$$

However, this model is restricted to a constant heating rate. In the applications of DAEM, it has been utilised to estimate the behaviour of different combinations of lignocellulosic biomass (pine wood) and polymer wastes (i.e., waste tyre, polylactic acid, PS, PET, PP, and HDPE) [34]. Besides that, this method has been incorporated into an ANN model to predict the pyrolytic properties of *Staghorn sumac* [106].

4.4 Optimisation methods

Optimisation methods or often referred to as heuristic models, such as genetic algorithm (GA), and particle swarm optimisation (PSO), shuffled complex evolution (SCE) are algorithms that could solve global optimization problems, i.e., for the pyrolysis process, the optimisation of the kinetic parameters to find the best fit using the data from the TGA. These optimisation methods generally solve problems by subjecting it to an objective function to determine the fitness of the iterations [109]. The objective functions or optimisation targets for a thermal degradation problem are the mass loss $\varnothing_{\mathrm{m}}$ and the mass loss rate $\varnothing_{\mathrm{mlr}}$ in Eqs. (12)–(14) as follows:

$$\varnothing=\varnothing_{\mathrm{m}}+\varnothing_{\mathrm{mlr}}, \tag{12}$$

$$\varnothing_{\mathrm{m}}=\sum_{j=1}^{N}\left[W_{CML,j}\frac{\sum_{k=1}^{n}(CML_{\mathrm{mod},k}-CML_{\exp,k})^2}{\sum_{k=1}^{n}\left(CML_{\exp,k}-\frac{1}{n}\sum_{p=1}^{n}CML_{\exp,p}\right)^2}\right], \tag{13}$$

$$\varnothing_{\mathrm{mlr}}=\sum_{j=1}^{N}\left[W_{MLR,j}\frac{\sum_{k=1}^{n}(MLR_{\mathrm{mod},k}-MLR_{\exp,k})^2}{\sum_{k=1}^{n}\left(MLR_{\exp,k}-\frac{1}{n}\sum_{p=1}^{n}MLR_{\exp,p}\right)^2}\right], \tag{14}$$

where CML_{mod} and CML_{exp} are the model and experimental cumulative mass loss, respectively; MLR_{mod} and MLR_{exp} are the model and experimental mass loss rate, respectively; N is the number of experiments, n is the number of data points for each experiment; and W_{CML} and W_{MLR} are the weighted value which can be defined as 1.

4.4.1 Genetic algorithm (GA)

The GA is based on an evolutionary concept to find the optimal solution to a complex problem globally. Firstly, the algorithm is initialised by carrying out a range search from a set of randomised candidate solutions referred to as a population. Each candidate solution is defined as an individual or a chromosome, containing the target parameters to be optimised (i.e., for the pyrolysis process, A, E_α and $\varnothing$), where the parameters are defined as genes in the GA [109]. Following the natural survival of the fittest, the population experience evolution forming subsequent generations according to the fitness of the objective function. Besides that, the new generation is produced by the chromosomes crossing over, exchanging information, and allowing mutation, this method helps to prevent the local optimal solution. Finally, by the process of elimination of relatively “unfit” candidate solution and reproducing generations that are “fit”. The application of GA in thermal degradation experiments are quite common, it is applied to solve the hybrid pyrolysis scheme of combining both parallel and convective first order reaction. Besides that, recent studies have combined it with different algorithms to improve the performance of the model, according to Aghbashlo et al. [110], the study combines GA with Adaptive Neuro–Fuzzy Interference System (ANFIS) achieving predictions of the kinetic parameters with better fitting compared to traditional ANFIS model; GA-least squares fitting procedure [111], where GA is applied to generate the initial guess for the least square function to solve for the optimal solution. This reduces the number of iterations required for the least square.

4.4.2 Particle swarm optimization (PSO)

The PSO algorithm follows the velocity and position search model. It contains a certain number of particles, their positions, and velocity. The particles in a particular position represent a candidate of solution of space, and the velocity of this particle updates the position of these particles [112]. In addition, these particles have a memory ability which, retains its historical best position vector and its global best position found [109]. Initially, the particles are assigned a random position and velocity in a proposed range. The solution then improves with iterations via Eqs. (15) and (16):

$$v_{id}^{k+1}=\omega v_{id}^{k}+c_1r_1\left(p_{id}-x_{id}^{k}\right)+c_2r_2\left(p_{gd}-x_{id}^{k}\right), \tag{15}$$

$$x_{id}^{k+1}=x_{id}^{k}+v_{id}^{k+1}, \tag{16}$$

where k is the iteration number, i is the particle number, and d is the search direction from 1 to D, w is the inertia weight, p_{id} and p_{gd} are the local particle position and the global best position of all particles, respectively. c_1 and c_2 are the two positive acceleration constants for the local and global nature of the swarm. r_1 and r_2 are the stochastic values in the range of [0,1], respectively [113,114].

According to Ding et al. [109], the study compares the performance between PSO and GA, and the results indicate that PSO showed closer global optimum convergence, 0.053 at the population size of 2500 compared to GA, with the best value at 0.075 at the population size of 2000. Besides that, PSO showed less fluctuation, 0.05 to 0.08 in fitting values regardless of population size, compared to GA, which fluctuates between 0.07 and 0.29. In literature, PSO is often coupled with other algorithms, such as global sensitivity analysis, to find the parameters with the greatest effect on the prediction outcome. According to Ding et al. [112], the sensitivity order is ranked from the largest to the smallest value which are representing the activation energy of lignin, the reaction order of cellulose, and the pre-exponential factor for lignin in the pyrolysis process of pinewood. While for the co-pyrolysis of microalgae *Chlorella vulgaris* and HDPE, the activation energy of cellulose, pre-exponential factor for cellulose and the activation energy of protein, followed by the reaction order of cellulose, showed significant influence on the prediction results, indicating these parameters should be paid much attention for the pyrolysis process [115]. Besides that, Monte Carlo simulations were applied to perform uncertainty analysis, to probabilistically assess the effects of stochastic uncertainties in the predictor values (n = 100000) from the ANN and PSO framework [113]. In addition, a recent study proposed a neuro-evolution algorithm, progressive deep swarm evolution (PDSE), built on the PSO algorithm, to model the catalytic thermal degradation of *Chlorella vulgaris* [88]. From the validation tests, implementing the PDSE algorithm obtained a coefficient of determination (R^2) value above 0.9990, RMSE below 0.0075, and MBE below 0.0026.

4.4.3 Shuffled complex evolution (SCE)

The SCE algorithm introduced by Duan et al. [116] is effective for calibration of hydrological models. The efficacy of this algorithm, a form of differential evolution (DE), comes from its use of geometric operations to find possible optimal solutions to space parameters. The algorithm solves global optimisation problems based on four concepts: (1) probabilistic and deterministic approaches; (2) clustering; (3) systematic evolution of a complex of points spanning the space in the direction of global improvement and (4) competitive evolution. The application of SCE on the woody pyrolysis was studied with six different kinetic models, comprising of single component reactant mechanism, and multicomponent reactant mechanisms (i.e., cellulose, hemicellulose, and lignin) [117]. The optimised kinetic parameters from the results were applied to predict the pyrolysis process with different heating rates, 5 and 80 °C·min^{-1}), where the results were found better fitting of the results of the multicomponent kinetic model, which can reach R^2 values of up to 0.99 [117]. Besides that, SCE has been applied in various pyrolysis kinetic analysis, pyrolysis of beech [118], and pyrolysis of basswood waste [119].

The SCE algorithm starts with generating of a population of random points within the search space, denoted as s. Each of these points contains a vector (i.e., kinetic parameters) and is ranked based on their fitness function value and stored in an array D, and partitioned into p complexes, each containing m points, i.e., $D = \{A^k, k = 1, ..., p\}$. Next, each complex evolved using the competitive complex evolution algorithm, and shuffled. All points are combined to a single population and the procedure of ranking for the function value, partition into complexes, evolution, and shuffling is repeated until convergence value is reached [116,120].

4.5 Predictive models: artificial neural network (ANN)

ANN is an intelligent learning, predictive computational technique, often employed to solve the nonlinear, and complex relationships between the input and output data. An ANN network consists of one or more hidden layers connecting the input (i) and output (o) layers. Each layer has a weight (w) matrix and an output vector [121]. The neuron of each single layer picks up the summation of the activation from the input vectors and their assigned weights and biases, the results then pass through an activation function (i.e., linear, sigmoid, and hyperbolic tangent sigmoid) to generate a new activation value to the neurons in the following layers. The weight matrix is altered to fit the learning algorithms, the learning ends when the weights of each layer achieve convergence as the final output vector (y_o) [122,123]. The ANN parameters influencing the performance are: the number of hidden layers (j), the number of neurons in each hidden layer (n), and the transfer function deployed denoted as f. The general architecture of the ANN is illustrated in Fig. 4.

Generally, the model learning process involves inputting a percentage of sample data to the network, and altering the number of neurons in the hidden layers to optimise the mean square error (MSE) [51]. Besides that, the selection is supervised by a learning algorithm. In literature, this method has been applied in predicting of the kinetic parameters of the pyrolysis process, involving the iso-conversional models, i.e., KAS and FWO shown in Table 7.

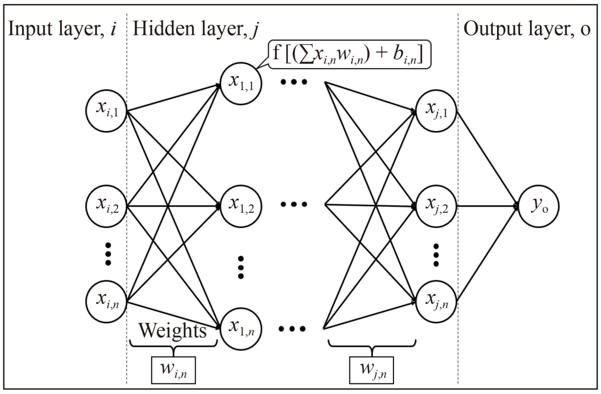

Fig. 4 General ANN architecture.

4.6 Thermodynamics relations

The thermodynamic parameters are important for the scale up and the design of the reactor, i.e., Frequency factor, A (s^{-1}), change in enthalpy, ΔH ($kJ \cdot mol^{-1}$), Gibbs free energy, ΔG ($kJ \cdot mol^{-1}$), and change in entropy, ΔS ($kJ \cdot mol^{-1} \cdot K^{-1}$). The parameters are expressed in the respective equations as Eqs. (17)–(20):

$$A = \frac{\beta \cdot E \cdot \exp\left(\dfrac{E}{R \cdot T_{\mathrm{m}}}\right)}{R \cdot T_{\mathrm{m}}^2}, \tag{17}$$

$$\Delta H = E_\alpha - R \cdot T, \tag{18}$$

$$\Delta G = E_\alpha + R \cdot T_{\mathrm{m}} \cdot \ln\left(\frac{K_{\mathrm{B}} \cdot T_{\mathrm{m}}}{h \cdot A}\right), \tag{19}$$

$$\Delta S = \frac{\Delta H - \Delta G}{T_{\mathrm{m}}}, \tag{20}$$

where T_{m}, K_{B}, h are the maximum temperature where the decomposition occurs (K), Boltzmann constant (1.381×10^{-23} $J \cdot K^{-1}$), and Plank's constant (6.626×10^{-34} $J \cdot s$) [30]. $A < 10^9$ s^{-1} refers to a simpler straightforward reaction, while $A > 10^9$ s^{-1} would mean the reaction follows a complex mechanism [129]. ΔH represents the endothermic or exothermic behaviour of the reaction mechanism; it is the amount of energy transferred during a chemical reaction. According to Gan et al. [130], the smaller the difference of ΔH with the E_α is, the more favourable for the reaction to occur. Hence, the bioenergy from the system is more likely to be attained. Moreover, ΔG is the total potential energy increased in the system, it signifies that the reactants are consumed and activated complexes are formed [21]. The ΔG also represents the suitability of the feedstock for pyrolysis, the higher the ΔG is, the more bioenergy can potentially be attained [30,51]. Furthermore, ΔS is the degree of arrangement of the carbon in the waste and biomass. It is the amount of energy unavailable to work. For higher entropy values, it indicates that the sample has yet to achieve thermodynamic equilibrium, and is highly reactive [131]. Table 8 summarises the kinetic and thermodynamic parameters for different feedstock samples.

5 Future outlooks

Many studies have proven that the combination of feedstock, biomass with waste plastic or biomass with waste tire in co-pyrolysis, with enhancements in the pyrolysis oil through synergistic effects, is an economical way for the production of sustainable fuel as a replacement for fossil fuels. The combination of waste plastics (20 wt %) with biomass generated a higher pyrolytic liquid yield compared to the solely thermal pyrolysis of biomass. This phenomenon shows that the oil produced from co-pyrolysis process can be blended with diesel after minor upgrading or even directly applied in transportation [132]. Nonetheless, not all plastic types can be applied in the process. In this sense, PVC, which consists of about 57% chlorine by weight, is not an ideal feedstock material as it will thermally break down into a very corrosive and toxic hydrochloric acid and influence the diesel quality with the production of chlorinated hydrocarbons. A 0.0145–0.0290 $mg \cdot m^{-3}$ of total chloride level has been recorded in the fuel oil product with just merely adding 1%–3% PVC in the feedstock stream [133,134]. Besides that, Hu et al. [32] stated that more studies are needed for co-pyrolysis especially in establishing a suitable approach in selecting material and the optimum blending ratio of material with biomass [32].

Furthermore, constraints in having straightforward and efficacious characterisation strategies for co-pyrolytic oil also impede the dependence of the industrial community in the technology [135]. Despite the extensive research works on the invention of the co-pyrolysis approach using

Table 7 ANN model compilation from different studies

Biomass/catalyst	Learning algorithm/ topology	Prediction result	ANN parameters	Ref.
Chlorella vulgaris limestone, HZSM-5	PDSE	Thermal degradation	Inputs: heating rate; heat flow; reactor temperature Outputs: remaining mass	[88]
Rice husk, sewage sludge	Levenberg–Marquardt (LM)	Thermal degradation	Inputs: reactor temperature; blend composition Outputs: mass loss	[21]
Chlorella vulgaris, peanut shell, microalgae ash	LM	Thermal degradation	Inputs: heating rate; reactor temperature Outputs: mass loss	[124]
Sewage sludge, peanut shell	LM	Thermal degradation	Inputs: blend compositions; heating rates; reactor temperature Outputs: remaining mass	[122]
Rice husk	Scaled conjugate gradient and LM	Thermal degradation	Inputs: heating rate; reactor temperature Outputs: remaining mass	[125]
Lignocellulosic biomass	Random forest schematic	Biochar yield	Dataset: physicochemical properties of lignocellulosic biomass	[126]
Sewage sludge	LM	HHV of syngas	Dataset: physicochemical properties of biomass	[127]
Mexican sunflower (*Tithonia diversifolia*)	LM	Bio-oil yield	Inputs: heating rate; flow rate; particle size; reactor temperature Output: bio-oil yield	[128]

Table 8 Kinetic and thermodynamic parameters of the pyrolysis process in literature

Feedstock	Catalyst	Kinetic model	E_α/ (kJ·mol^{-1})	A/ min^{-1}	ΔH/ (kJ·mol^{-1})	ΔS/ (J·mol^{-1}·K^{-1})	ΔG/ (kJ·mol^{-1})	Ref.
Pterocarpus indicus	–	Coats-redfern	112.0	–	103.0	–138.0	183.00	[35]
Intsia bijuga	–		99.0	–	89.0	–120.0	160.00	
Corn stover	–		66.0	–	57.0	–173.0	147.00	
HDPE	–		546.0	–	533.0	420.0	226.00	
LDPE	–		487.0	–	475.0	348.0	231.00	
PP	–		423.0	–	411.0	273.0	222.00	
Rice hull	–	DAEM	175.4	2.939×10^{17}	170.2	–	–	[130]
	–	FWO	177.7	7.991×10^{16}	172.6	–	–	
	Limestone	DAEM	123.3	5.803×10^{11}	117.9	–	–	
	Limestone	FWO	132.5	4.148×10^{12}	127.1	–	–	
	Eggshell	DAEM	96.1	2.033×10^{10}	90.8	–	–	
	Eggshell	FWO	100.4	1.948×10^{9}	95.2	–	–	
Sewage sludge (97.5% conversion)	–	KAS	123.6	1.440×10^{6}	119.5	139.4	187.69	[51]
	–	FWO	132.7	1.560×10^{9}	128.6	138.8	196.50	
	–	Friedman	92.4	0.0103	88.3	295.4	232.80	
	–	Popescu	200.9	9.740×10^{10}	196.8	219.3	304..00	
Microalgae:microalgae ash:peanut shell 9:2:9	–	FWO	142.6	2.010×10^{14}	137.0	–	–	[124]
Garlic husk	–	KAS	154.0	–	149.4	–	150.60	[104]
	–	FWO	154.9	–	150.4	–	150.50	
	–	Starink	154.3	–	149.8	–	150.50	
Staghorn sumac	–	FWO	167.9	–	178.9	–	–	[106]
	–	KAS	169.4	–	167.2	–	–	
	–	Starink	169.8	–	167.6	–	–	
Azadirachta indica	–	FWO	–	6.288×10^{15}	188.5	–43.3	215.40	[30]
	–	Friedman	–	8.586×10^{15}	190.9	–39.4	215.40	
	–	Vyazovkin	–	2.965×10^{20}	199.7	–26.0	215.20	
Phyllantus emblica	–	FWO	–	2.075×10^{14}	189.9	–40.9	215.30	[30]
	–	Friedman	–	2.864×10^{13}	181.3	–55.1	215.60	
	–	Vyazovkin	–	3.534×10^{13}	179.4	–58.3	215.60	
Rice husk	–	Friedman	–	–	186	–	–	[92]
	–	KAS	–	–	178	–	–	
	–	FWO	–	–	180	–	–	
	Rice hull ash	Friedman	–		148	–	–	
	Rice hull ash	KAS	–	–	148	–	–	
	Rice hull ash	FWO	–	–	146	–	–	
Chlorella vulgaris	–	KAS	156.2	2.898×10^{20}	151	–	–	[131]
	–	FWO	158.1	2.358×10^{20}	153	–	–	
	HZSM-5	KAS	145.3	2.790×10^{14}	140	–	–	
	HZSM-5	FWO	147.8	4.908×10^{14}	143	–	–	
	Limestone	KAS	138.8	6.360×10^{15}	133	–	–	
	Limestone	FWO	142.1	8.880×10^{15}	137	–	–	

different kinds of agricultural biomass and polymer wastes, the current heat transfer processes for co-pyrolysis, i.e., conduction, convection and radiation still impose several challenges. In conduction, solid attrition is the critical issue once there is a direct contact between fuel particles and heating agent. In convection, small fuel particles and long gas residence times are essential for gas/solid and sufficient heat transfer, respectively. Asymmetrically, the primary challenges of radiation are high concentration of radiation is required for the production of sufficient heat transfer and consideration of wall heating design in pyrolysis reactor [136,137]. Hence, the high installation and operating costs of units with a high efficiency of heat transfer in the short gas residence time and an additional pre-treatment system for various types of biomasses are the main drawbacks of co-pyrolysis. Different studies reported that different conditions are required to blend an appropriate waste with different biomasses before co-processing. More profound fundamental studies on reaction mechanisms and kinetics of biomass with different waste materials are critical in the advancement of the co-pyrolysis process. In this sense, the properties of the co-pyrolytic oil produced with its composition can be determined from the interactivity of the reaction intermediates. Currently, ANN and Monte Carlo serve as empirical models that are practical in the prediction of intricate input–output interrelations in a co-pyrolysis process. However, these models are only applicable to the process and fuels, which have been well-established [21]. Co-pyrolysis kinetic datasets for predicting of product formation using different reactor systems are still fairly unexplored [135].

Moreover, the commercialisation of co-pyrolysis reactors are still in the early stages since the current reactors still have the challenges of low heat efficiency, high capital and operating costs as well as complexities with biomass handling or storage [32]. Besides that, although there is plenty of extensive research on the single feedstock pyrolysis, the feasibility study of the co-pyrolysis process remains a niche area, whereby research on the techno-economic and life cycle assessment of the process is limited to single feedstock pyrolysis, such as the co-pyrolysis of biomass refineries and the DFM layers in these references [138,139]. To the best of our knowledge, these studies for the case of co-pyrolysis are scarce, existing studies focus on the microwave co-pyrolysis of food waste and LDPE [140], and the co-pyrolysis of lignite coal with single-use plastic waste [141]. Besides that, the existing research on the modelling of the co-pyrolysis of biomass with plastic waste reaction kinetics has been widely studied, but yet to have a consensus on the reaction pathway [32].

6 Conclusions

To conclude, the recent technologies and techniques of co-pyrolysis of biomass and plastic waste to produce bio-oil have been summarised in this review. The growing agriculture industry in ASEAN countries to suit the growing population of the region, has subsequently generated landfills of biomass. To exacerbate the situation, the global pandemic gives rise to the surge of the single-use plastic waste, DMFM wastes. Fortunately, the exploitation of these wastes in co-pyrolysis would positively improve the quantity and quality of the extracted bio-oil of the process, as the result of the synergistic interactions between lignocellulosic properties of biomass and the high hydrogen content of the plastic wastes. Furthermore, the advancement of the kinetic analysis of the pyrolysis process has improved as the catalytic co-pyrolysis process becomes more complex, and unable to be explained via simple iso-conversional models. Advanced conversional models such as Vyazovkin and DAEM methods have been introduced to study the pyrolysis reaction, followed by the heuristic model and predictive models, which prove to produce high-accuracy results. However, the studies of co-pyrolysis of biomass and DMFMs remain limited. Experimental work on the binary feedstock's thermal decompositions and the bio-oil product's quantity and quality result from the co-pyrolysis has yet to be clear. The proposal of this methodology could serve as potential solution to help reduce or eliminate the pollution caused by the DMFM wastes, while producing value-added bio-oil products.

Acknowledgements The authors would like to acknowledge the technical support from Curtin University Malaysia, Swinburne University of Technology, Universiti Teknologi PETRONAS (UTP), and Manipal University Jaipur. Besides that, M.X.J. Wee would like to acknowledge the full funding support from the Curtin Malaysia Postgraduate Research Studentship (CMPRS) for the PhD study.

References

1. Adnan Z A, Saniayan V. Renewable energy outlook for ASEAN: a REmap analysis. Asean Centre for Energy & IRENA Report, 2016
2. Miranda M. Governments across Southeast Asia accelerate renewable energy investment to revive the pandemic-hit economies. Power Technology Report, 2020
3. Erdiwansyah M, Mamat R, Sani M S M, Khoerunnisa F, Kadarohman A. Target and demand for renewable energy across 10 ASEAN countries by 2040. Electricity Journal, 2019, 32(10): 106670
4. Sarraf M, Rismanchi B, Saidur R, Ping H W, Rahim N A. Renewable energy policies for sustainable development in Cambodia. Renewable & Sustainable Energy Reviews, 2013, 22: 223–229
5. Pillai I R, Banerjee R. Renewable energy in India: status and potential. Energy, 2009, 34(8): 970–980
6. Dani S, Wibawa A. Challenges and policy for biomass energy in Indonesia. Journal of International Economic Law, 2018, 15(5): 41–47
7. Mekhilef S, Barimani M, Safari A, Salam Z. Malaysia's renewable energy policies and programs with green aspects. Renewable & Sustainable Energy Reviews, 2014, 40: 497–504
8. Wattana S. Bioenergy development in Thailand: challenges and strategies. Energy Procedia, 2014, 52: 506–515
9. Truong K, Huong C, Dang Xuan T, Trung D, Khanh T. Current status and future plan of development of bioenergy crops as renewable energy sources in Vietnam. Journal of Biology and Nature, 2016, 5: 1–8
10. Myanmar Energy Master Plan. IEA, 2017
11. Energy policy and administration. Open Development Laos Website, 2018
12. Bangkok. East and Southeast Asia renewable energy statistics workshop. IRENA Website, 2016
13. Hirschmann R. Palm oil industry in Indonesia—statistics & facts. Statista Website, 2022
14. Malaysia palm oil production by year. Indexmundi, 2020
15. Loh S K. The potential of the Malaysian oil palm biomass as a renewable energy source. Energy Conversion and Management, 2017, 141: 285–298

16. Kumar N, Chhokar R S, Meena R P, Kharub A S, Gill S C, Tripathi S C, Gupta O P, Mangrauthia S K, Sundaram R M, Sawant C P, Gupta A, Naorem A, Kumar M, Singh G P. Challenges and opportunities in productivity and sustainability of rice cultivation system: a critical review in Indian perspective. Cereal Research Communications, 2022, 50: 573–601
17. Dai L, Wang Y, Liu Y, He C, Ruan R, Yu Z, Jiang L, Zeng Z, Wu Q. A review on selective production of value-added chemicals via catalytic pyrolysis of lignocellulosic biomass. Science of the Total Environment, 2020, 749: 142386
18. Kan T, Strezov V, Evans T, He J, Kumar R, Lu Q. Catalytic pyrolysis of lignocellulosic biomass: a review of variations in process factors and system structure. Renewable & Sustainable Energy Reviews, 2020, 134: 110305
19. Sivagurunathan P, Raj T, Mohanta C S, Semwal S, Satlewal A, Gupta R P, Puri S K, Ramakumar S S V, Kumar R. 2G waste lignin to fuel and high value-added chemicals: approaches, challenges and future outlook for sustainable development. Chemosphere, 2021, 268: 129326
20. Yang H, Yan R, Chen H, Lee D H, Liang D T, Zheng C. Pyrolysis of palm oil wastes for enhanced production of hydrogen rich gases. Fuel Processing Technology, 2006, 87(10): 935–942
21. Naqvi S R, Hameed Z, Tariq R, Taqvi S A, Ali I, Niazi M B K, Noor T, Hussain A, Iqbal N, Shahbaz M. Synergistic effect on co-pyrolysis of rice husk and sewage sludge by thermal behavior, kinetics, thermodynamic parameters and artificial neural network. Waste Management, 2019, 85: 131–140
22. Suriapparao D V, Vinu R, Shukla A, Haldar S. Effective deoxygenation for the production of liquid biofuels via microwave assisted co-pyrolysis of agro residues and waste plastics combined with catalytic upgradation. Bioresource Technology, 2020, 302: 122775
23. Geyer R, Jambeck J R, Law K L. Production, use, and fate of all plastics ever made. Science Advances, 2017, 3(7): e1700782
24. Jambeck J R, Geyer R, Wilcox C, Siegler T R, Perryman M, Andrady A, Narayan R, Law K L. Plastic waste inputs from land into the ocean. Science, 2015, 347(6223): 768–771
25. Abnisa F, Alaba P A. Recovery of liquid fuel from fossil-based solid wastes via pyrolysis technique: a review. Journal of Environmental Chemical Engineering, 2021, 9(6): 106593
26. Liang Y, Song Q, Wu N, Li J, Zhong Y, Zeng W. Repercussions of COVID-19 pandemic on solid waste generation and management strategies. Frontiers of Environmental Science & Engineering, 2021, 15(6): 115
27. Chaib F. Shortage of personal protective equipment endangering health workers worldwide. World Health Organization Website, 2020
28. Patrício Silva A L, Prata J C, Duarte A C, Barcelò D, Rocha-Santos T. An urgent call to think globally and act locally on landfill disposable plastics under and after Covid-19 pandemic: pollution prevention and technological (Bio) remediation solutions. Chemical Engineering Journal, 2021, 426: 131201
29. Patrício Silva A L, Prata J C, Mouneyrac C, Barcelò D, Duarte A C, Rocha-Santos T. Risks of Covid-19 face masks to wildlife: present and future research needs. Science of the Total Environment, 2021, 792: 148505
30. Mishra R K, Mohanty K. Kinetic analysis and pyrolysis behaviour of waste biomass towards its bioenergy potential. Bioresource Technology, 2020, 311: 123480
31. Akhtar J, Saidina Amin N. A review on operating parameters for optimum liquid oil yield in biomass pyrolysis. Renewable & Sustainable Energy Reviews, 2012, 16(7): 5101–5109
32. Hu X, Gholizadeh M. Biomass pyrolysis: a review of the process development and challenges from initial researches up to the commercialisation stage. Journal of Energy Chemistry, 2019, 39: 109–143
33. Miandad R, Barakat M A, Rehan M, Aburiazaiza A S, Ismail I M I, Nizami A S. Plastic waste to liquid oil through catalytic pyrolysis using natural and synthetic zeolite catalysts. Waste Management, 2017, 69: 66–78
34. Navarro M V, López J M, Veses A, Callén M S, García T. Kinetic study for the co-pyrolysis of lignocellulosic biomass and plastics using the distributed activation energy model. Energy, 2018, 165: 731–742
35. Salvilla J N V, Ofrasio B I G, Rollon A P, Manegdeg F G, Abarca R R M, de Luna M D G. Synergistic co-pyrolysıs of polyolefin plastics with wood and agricultural wastes for biofuel production. Applied Energy, 2020, 279: 115668
36. Wang L, Chai M, Liu R, Cai J. Synergetic effects during co-pyrolysis of biomass and waste tire: a study on product distribution and reaction kinetics. Bioresource Technology, 2018, 268: 363–370
37. Ansari K B, Hassan S Z, Bhoi R, Ahmad E. Co-pyrolysis of biomass and plastic wastes: a review on reactants synergy, catalyst impact, process parameter, hydrocarbon fuel potential, COVID-19. Journal of Environmental Chemical Engineering, 2021, 9(6): 106436
38. Roy P, Dias G. Prospects for pyrolysis technologies in the bioenergy sector: a review. Renewable & Sustainable Energy Reviews, 2017, 77: 59–69
39. Bridgwater A V. Review of fast pyrolysis of biomass and product upgrading. Biomass and Bioenergy, 2012, 38: 68–94
40. Fahmy T Y A, Fahmy Y, Mobarak F, El-Sakhawy M, Abou-Zeid R E. Biomass pyrolysis: past, present, and future. Environment, Development and Sustainability, 2020, 22(1): 17–32
41. Papari S, Hawboldt K. A review on the pyrolysis of woody biomass to bio-oil: focus on kinetic models. Renewable & Sustainable Energy Reviews, 2015, 52: 1580–1595
42. Perkins G, Bhaskar T, Konarova M. Process development status of fast pyrolysis technologies for the manufacture of renewable transport fuels from biomass. Renewable & Sustainable Energy Reviews, 2018, 90: 292–315
43. Foong S Y, Liew R K, Yang Y, Cheng Y W, Yek P N Y, Wan Mahari W A, Lee X Y, Han C S, Vo D V N, Van Le Q, Aghbashlo M, Tabatabaei M, Sonne C, Peng W, Lam S S. Valorization of biomass waste to engineered activated biochar by microwave pyrolysis: progress, challenges, and future directions. Chemical Engineering Journal, 2020, 389: 124401
44. Tsai F M, Bui T D, Tseng M L, Lim M K, Hu J. Municipal solid waste management in a circular economy: a data-driven

bibliometric analysis. Journal of Cleaner Production, 2020, 275: 124132

45. Andreo-Martínez P, Ortiz-Martínez V M, García-Martínez N, de los Ríos A P, Hernández-Fernández F J, Quesada-Medina J. Production of biodiesel under supercritical conditions: state of the art and bibliometric analysis. Applied Energy, 2020, 264: 114753
46. Losse M, Geissdoerfer M. Mapping socially responsible investing: a bibliometric and citation network analysis. Journal of Cleaner Production, 2021, 296: 126376
47. Murillo J, Villegas L M, Ulloa-Murillo L M, Rodríguez A R. Recent trends on omics and bioinformatics approaches to study SARS-CoV-2: a bibliometric analysis and mini-review. Computers in Biology and Medicine, 2021, 128: 104162
48. Bensidhom G, Ben Hassen Trabelsi A, mahmood M A, Ceylan S. mahmood M A, Ceylan S. Insights into pyrolytic feedstock potential of date palm industry wastes: kinetic study and product characterization. Fuel, 2021, 285: 119096
49. Domínguez A, Menéndez J A, Inguanzo M, Pis J J. Investigations into the characteristics of oils produced from microwave pyrolysis of sewage sludge. Fuel Processing Technology, 2005, 86(9): 1007–1020
50. Ghodke P, Mandapati R N. Investigation of particle level kinetic modeling for babul wood pyrolysis. Fuel, 2019, 236: 1008–1017
51. Naqvi S R, Tariq R, Hameed Z, Ali I, Taqvi S A, Naqvi M, Niazi M B K, Noor T, Farooq W. Pyrolysis of high-ash sewage sludge: thermo-kinetic study using TGA and artificial neural networks. Fuel, 2018, 233: 529–538
52. Polin J P, Carr H D, Whitmer L E, Smith R G, Brown R C. Conventional and autothermal pyrolysis of corn stover: overcoming the processing challenges of high-ash agricultural residues. Journal of Analytical and Applied Pyrolysis, 2019, 143: 104679
53. Singh R K, Pandey D, Patil T, Sawarkar A N. Pyrolysis of banana leaves biomass: physico-chemical characterization, thermal decomposition behavior, kinetic and thermodynamic analyses. Bioresource Technology, 2020, 310: 123464
54. Tabal A, Barakat A, Aboulkas A, El harfi K. Pyrolysis of ficus nitida wood: determination of kinetic and thermodynamic parameters. Fuel, 2021, 283: 119253
55. Ding Z, Chen H, Liu J, Cai H, Evrendilek F, Buyukada M. Pyrolysis dynamics of two medical plastic wastes: drivers, behaviors, evolved gases, reaction mechanisms, and pathways. Journal of Hazardous Materials, 2021, 402: 123472
56. Honus S, Kumagai S, Fedorko G, Molnár V, Yoshioka T. Pyrolysis gases produced from individual and mixed PE, PP, PS, PVC, and PET—Part I: Production and physical properties. Fuel, 2018, 221: 346–360
57. Jeon W, Kim Y D, Lee K H. A comparative study on pyrolysis of bundle and fluffy shapes of waste packaging plastics. Fuel, 2021, 283: 119260
58. Jung S, Lee S, Dou X, Kwon E E. Valorization of disposable COVID-19 mask through the thermo-chemical process. Chemical Engineering Journal, 2021, 405: 126658
59. Parku G K, Collard F X, Görgens J F. Pyrolysis of waste polypropylene plastics for energy recovery: influence of heating rate and vacuum conditions on composition of fuel product. Fuel Processing Technology, 2020, 209: 106522
60. Xu F, Wang B, Yang D, Hao J, Qiao Y, Tian Y. Thermal degradation of typical plastics under high heating rate conditions by TG-FTIR: pyrolysis behaviors and kinetic analysis. Energy Conversion and Management, 2018, 171: 1106–1115
61. Park Y K, Ha J M, Oh S, Lee J. Bio-oil upgrading through hydrogen transfer reactions in supercritical solvents. Chemical Engineering Journal, 2021, 404: 126527
62. Kwon D, Jung S, Lin K Y A, Tsang Y F, Park Y K, Kwon E E. Synergistic effects of CO_2 on complete thermal degradation of plastic waste mixture through a catalytic pyrolysis platform: a case study of disposable diaper. Journal of Hazardous Materials, 2021, 419: 126537
63. Wan Mahari W A, Awang S, Zahariman N A Z, Peng W, Man M, Park Y K, Lee J, Sonne C, Lam S S. Microwave co-pyrolysis for simultaneous disposal of environmentally hazardous hospital plastic waste, lignocellulosic, and triglyceride biowaste. Journal of Hazardous Materials, 2022, 423: 127096
64. Park Y K, Lee B, Lee H W, Watanabe A, Jae J, Tsang Y F, Kim Y M. Co-feeding effect of waste plastic films on the catalytic pyrolysis of *Quercus variabilis* over microporous HZSM-5 and HY catalysts. Chemical Engineering Journal, 2019, 378: 122151
65. Hu Y, Yu W, Wibowo H, Xia Y, Lu Y, Yan M. Effect of catalysts on distribution of polycyclic-aromatic hydrocarbon (PAHs) in bio-oils from the pyrolysis of dewatered sewage sludge at high and low temperatures. Science of the Total Environment, 2019, 667: 263–270
66. Zhang X, Lei H, Zhu L, Zhu X, Qian M, Yadavalli G, Wu J, Chen S. Thermal behavior and kinetic study for catalytic co-pyrolysis of biomass with plastics. Bioresource Technology, 2016, 220: 233–238
67. Lin X, Zhang Z, Wang Q, Sun J. Interactions between biomass-derived components and polypropylene during wood-plastic composite pyrolysis. Biomass Conversion and Biorefinery, 2020, 12(8): 3345–3357
68. Önal E, Uzun B B, Pütün A E. Bio-oil production via co-pyrolysis of almond shell as biomass and high density polyethylene. Energy Conversion and Management, 2014, 78: 704–710
69. Sun J, Luo J, Lin J, Ma R, Sun S, Fang L, Li H. Study of co-pyrolysis endpoint and product conversion of plastic and biomass using microwave thermogravimetric technology. Energy, 2022, 247: 123547
70. Yang J, Rizkiana J, Widayatno W B, Karnjanakom S, Kaewpanha M, Hao X, Abudula A, Guan G. Fast co-pyrolysis of low density polyethylene and biomass residue for oil production. Energy Conversion and Management, 2016, 120: 422–429
71. Ojha D, Shukla S, Raghunath S, Sachin R S, Vinu R. Understanding the interactions between cellulose and polypropylene during fast co-pyrolysis via experiments and DFT calculations. Chemical Engineering Transactions, 2016, 50: 67–72
72. Uzoejinwa B B, He X, Wang S, El-Fatah Abomohra A, Hu Y, Wang Q. Co-pyrolysis of biomass and waste plastics as a thermochemical conversion technology for high-grade biofuel

production: recent progress and future directions elsewhere worldwide. Energy Conversion and Management, 2018, 163: 468–492

73. Lin X, Kong L, Ren X, Zhang D, Cai H, Lei H. Catalytic co-pyrolysis of torrefied poplar wood and high-density polyethylene over hierarchical HZSM-5 for mono-aromatics production. Renewable Energy, 2021, 164: 87–95
74. Pogaku R, Hardinge B S, Vuthaluru H, Amir H A. Production of bio-oil from oil palm empty fruit bunch by catalytic fast pyrolysis: a review. Biofuels, 2016, 7(6): 647–660
75. Dai L, Zhou N, Li H, Deng W, Cheng Y, Wang Y, Liu Y, Cobb K, Lei H, Chen P, Ruan R. Recent advances in improving lignocellulosic biomass-based bio-oil production. Journal of Analytical and Applied Pyrolysis, 2020, 149: 104845
76. Yang H, Yan R, Chin T, Liang D T, Chen H, Zheng C. Thermogravimetric analysis-fourier transform infrared analysis of palm oil waste pyrolysis. Energy & Fuels, 2004, 18(6): 1814–1821
77. Ly H V, Park J W, Kim S S, Hwang H T, Kim J, Woo H C. Catalytic pyrolysis of bamboo in a bubbling fluidized-bed reactor with two different catalysts: HZSM-5 and red mud for upgrading bio-oil. Renewable Energy, 2020, 149: 1434–1445
78. Ahmed M H M, Batalha N, Mahmudul H M D, Perkins G, Konarova M. A review on advanced catalytic co-pyrolysis of biomass and hydrogen-rich feedstock: insights into synergistic effect, catalyst development and reaction mechanism. Bioresource Technology, 2020, 310: 123457
79. Jin X, Lee J H, Choi J W. Catalytic co-pyrolysis of woody biomass with waste plastics: effects of HZSM-5 and pyrolysis temperature on producing high-value pyrolytic products and reducing wax formation. Energy, 2022, 239: 121739
80. Ratnasari D K, Nahil M A, Williams P T. Catalytic pyrolysis of waste plastics using staged catalysis for production of gasoline range hydrocarbon oils. Journal of Analytical and Applied Pyrolysis, 2017, 124: 631–637
81. Li Z, Zhong Z, Zhang B, Wang W, Seufitelli G V S, Resende F L P. Catalytic fast co-pyrolysis of waste greenhouse plastic films and rice husk using hierarchical micro-mesoporous composite molecular sieve. Waste Management, 2020, 102: 561–568
82. Zhao Y, Wang Y, Duan D, Ruan R, Fan L, Zhou Y, Dai L, Lv J, Liu Y. Fast microwave-assisted ex-catalytic co-pyrolysis of bamboo and polypropylene for bio-oil production. Bioresource Technology, 2018, 249: 69–75
83. Cao Z, Niu J, Gu Y, Zhang R, Liu Y, Luo L. Catalytic pyrolysis of rice straw: screening of various metal salts, metal basic oxide, acidic metal oxide and zeolite catalyst on products yield and characterization. Journal of Cleaner Production, 2020, 269: 122079
84. Chen X, Chen Y, Yang H, Chen W, Wang X, Chen H. Fast pyrolysis of cotton stalk biomass using calcium oxide. Bioresource Technology, 2017, 233: 15–20
85. Chong Y Y, Thangalazhy-Gopakumar S, Ng H K, Lee L Y, Gan S. Effect of oxide catalysts on the properties of bio-oil from in-situ catalytic pyrolysis of palm empty fruit bunch fiber. Journal of Environmental Management, 2019, 247: 38–45
86. Kim S, Park C, Lee J. Reduction of polycyclic compounds and biphenyls generated by pyrolysis of industrial plastic waste by using supported metal catalysts: a case study of polyethylene terephthalate treatment. Journal of Hazardous Materials, 2020, 392: 122464
87. Lin X, Zhang Z, Zhang Z, Sun J, Wang Q, Pittman C U. Catalytic fast pyrolysis of a wood-plastic composite with metal oxides as catalysts. Waste Management, 2018, 79: 38–47
88. Teng S Y, Loy A C M, Leong W D, How B S, Chin B L F, Máša V. Catalytic thermal degradation of *Chlorella vulgaris*: evolving deep neural networks for optimization. Bioresource Technology, 2019, 292: 121971
89. Thangalazhy-Gopakumar S, Wei Lee C, Gan S, Kiat Ng H, Yee Lee L. Comparison of bio-oil properties from non-catalytic and in-situ catalytic fast pyrolysis of palm empty fruit bunch. Materials Today: Proceedings, 2018, 5(11): 23456–23465
90. Chow L W, Tio S A, Teoh J Y, Lim C G, Chong Y Y, Thangalazhy-Gopakumar S. Sludge as a relinquishing catalyst in co-pyrolysis with palm empty fruit bunch fiber. Journal of Analytical and Applied Pyrolysis, 2018, 132: 56–64
91. Jeong J Y, Lee U D, Chang W S, Jeong S H. Production of bio-oil rich in acetic acid and phenol from fast pyrolysis of palm residues using a fluidized bed reactor: influence of activated carbons. Bioresource Technology, 2016, 219: 357–364
92. Loy A C M, Gan D K W, Yusup S, Chin B L F, Lam M K, Shahbaz M, Unrean P, Acda M N, Rianawati E. Thermogravimetric kinetic modelling of *in-situ* catalytic pyrolytic conversion of rice husk to bioenergy using rice hull ash catalyst. Bioresource Technology, 2018, 261: 213–222
93. Loy A C M, Yusup S, Lam M K, Chin B L F, Shahbaz M, Yamamoto A, Acda M N. The effect of industrial waste coal bottom ash as catalyst in catalytic pyrolysis of rice husk for syngas production. Energy Conversion and Management, 2018, 165: 541–554
94. Santosa D M, Zhu C, Agblevor F A, Maddi B, Roberts B Q, Kutnyakov I V, Lee S J, Wang H. *In situ* catalytic fast pyrolysis using red mud catalyst: impact of catalytic fast pyrolysis temperature and biomass feedstocks. ACS Sustainable Chemistry & Engineering, 2020, 8(13): 5156–5164
95. Dong Q, Li H, Niu M, Luo C, Zhang J, Qi B, Li X, Zhong W. Microwave pyrolysis of moso bamboo for syngas production and bio-oil upgrading over bamboo-based biochar catalyst. Bioresource Technology, 2018, 266: 284–290
96. Chen W, Fang Y, Li K, Chen Z, Xia M, Gong M, Chen Y, Yang H, Tu X, Chen H. Bamboo wastes catalytic pyrolysis with N-doped biochar catalyst for phenols products. Applied Energy, 2020, 260: 114242
97. An Y, Tahmasebi A, Zhao X, Matamba T, Yu J. Catalytic reforming of palm kernel shell microwave pyrolysis vapors over iron-loaded activated carbon: enhanced production of phenol and hydrogen. Bioresource Technology, 2020, 306: 123111
98. Gaurh P, Pramanik H. Production of benzene/toluene/ethyl benzene/xylene (BTEX) via multiphase catalytic pyrolysis of hazardous waste polyethylene using low cost fly ash synthesized natural catalyst. Waste Management, 2018, 77: 114–130
99. Luo W, Fan Z, Wan J, Hu Q, Dong H, Zhang X, Zhou Z. Study on the reusability of kaolin as catalysts for catalytic pyrolysis of

low-density polyethylene. Fuel, 2021, 302: 121164

100. Nalluri P, Prem Kumar P, Ch Sastry M R. Experimental study on catalytic pyrolysis of plastic waste using low cost catalyst. Materials Today: Proceedings, 2021, 45: 7216–7221
101. Xu D, Xiong Y, Zhang S, Su Y. The synergistic mechanism between coke depositions and gas for H_2 production from co-pyrolysis of biomass and plastic wastes via char supported catalyst. Waste Management, 2021, 121: 23–32
102. Zhang D, Lin X, Zhang Q, Ren X, Yu W, Cai H. Catalytic pyrolysis of wood-plastic composite waste over activated carbon catalyst for aromatics production: effect of preparation process of activated carbon. Energy, 2020, 212: 118983
103. Chang G, Shi P, Guo Y, Wang L, Wang C, Guo Q. Enhanced pyrolysis of palm kernel shell wastes to bio-based chemicals and syngas using red mud as an additive. Journal of Cleaner Production, 2020, 272: 122847
104. Singh R K, Patil T, Sawarkar A N. Pyrolysis of garlic husk biomass: physico-chemical characterization, thermodynamic and kinetic analyses. Bioresource Technology Reports, 2020, 12: 100558
105. Sbirrazzuoli N. Determination of pre-exponential factors and of the mathematical functions $f(\alpha)$ or $G(\alpha)$ that describe the reaction mechanism in a model-free way. Thermochimica Acta, 2013, 564: 59–69
106. Sajjad Ahmad M, Liu H, Alhumade H, Hussain Tahir M, Çakman G, Yıldız A, Ceylan S, Elkamel A, Shen B. A modified DAEM: to study the bioenergy potential of invasive *Staghorn sumac* through pyrolysis, ANN, TGA, kinetic modeling, FTIR and GC-MS analysis. Energy Conversion and Management, 2020, 221: 113173
107. Hameed S, Sharma A, Pareek V, Wu H, Yu Y. A review on biomass pyrolysis models: kinetic, network and mechanistic models. Biomass and Bioenergy, 2019, 123: 104–122
108. Cano-Pleite E, Rubio-Rubio M, García-Hernando N, Soria-Verdugo A. Microalgae pyrolysis under isothermal and non-isothermal conditions. Algal Research, 2020, 51: 102031
109. Ding Y, Zhang W, Yu L, Lu K. The accuracy and efficiency of GA and PSO optimization schemes on estimating reaction kinetic parameters of biomass pyrolysis. Energy, 2019, 176: 582–588
110. Aghbashlo M, Almasi F, Jafari A, Nadian M H, Soltanian S, Lam S S, Tabatabaei M. Describing biomass pyrolysis kinetics using a generic hybrid intelligent model: a critical stage in sustainable waste-oriented biorefineries. Renewable Energy, 2021, 170: 81–91
111. Ferreiro A I, Rabaçal M, Costa M. A combined genetic algorithm and least squares fitting procedure for the estimation of the kinetic parameters of the pyrolysis of agricultural residues. Energy Conversion and Management, 2016, 125: 290–300
112. Ding Y, Zhang Y, Zhang J, Zhou R, Ren Z, Guo H. Kinetic parameters estimation of pinus sylvestris pyrolysis by Kissinger–Kai method coupled with particle swarm optimization and global sensitivity analysis. Bioresource Technology, 2019, 293: 122079
113. Buyukada M. Co-combustion of peanut hull and coal blends: artificial neural networks modeling, particle swarm optimization and Monte Carlo simulation. Bioresource Technology, 2016, 216: 280–286
114. Xu L, Jiang Y, Wang L. Thermal decomposition of rape straw: pyrolysis modeling and kinetic study via particle swarm optimization. Energy Conversion and Management, 2017, 146: 124–133
115. Majid M, Chin B L F, Jawad Z A, Chai Y H, Lam M K, Yusup S, Cheah K W. Particle swarm optimization and global sensitivity analysis for catalytic co-pyrolysis of *Chlorella vulgaris* and plastic waste mixtures. Bioresource Technology, 2021, 329: 124874
116. Duan Q Y, Gupta V K, Sorooshian S. Shuffled complex evolution approach for effective and efficient global minimization. Journal of Optimization Theory and Applications, 1993, 76(3): 501–521
117. Ding Y, Zhang J, He Q, Huang B, Mao S. The application and validity of various reaction kinetic models on woody biomass pyrolysis. Energy, 2019, 179: 784–791
118. Ding Y, Wang C, Chaos M, Chen R, Lu S. Estimation of beech pyrolysis kinetic parameters by Shuffled Complex Evolution. Bioresource Technology, 2016, 200: 658–665
119. Liu H, Chen B, Wang C. Pyrolysis kinetics study of biomass waste using Shuffled Complex Evolution algorithm. Fuel Processing Technology, 2020, 208: 106509
120. Hasalová L, Ira J, Jahoda M. Practical observations on the use of Shuffled Complex Evolution (SCE) algorithm for kinetic parameters estimation in pyrolysis modeling. Fire Safety Journal, 2016, 80: 71–82
121. Al-Yaari M, Ibrahim D. Application of artificial neural networks to predict the catalytic pyrolysis of HDPE using non-isothermal TGA data. Polymers, 2020, 12(8): 1813
122. Bi H, Wang C, Jiang X, Jiang C, Bao L, Lin Q. Thermodynamics, kinetics, gas emissions and artificial neural network modeling of co-pyrolysis of sewage sludge and peanut shell. Fuel, 2021, 284: 118988
123. Balsora H K, S K, Dua V, Joshi J B, Kataria G, Sharma A, Chakinala A G. Machine learning approach for the prediction of biomass pyrolysis kinetics from preliminary analysis. Journal of Environmental Chemical Engineering, 2022, 10(3): 108025
124. Bong J T, Loy A C M, Chin B L F, Lam M K, Tang D K H, Lim H Y, Chai Y H, Yusup S. Artificial neural network approach for co-pyrolysis of *Chlorella vulgaris* and peanut shell binary mixtures using microalgae ash catalyst. Energy, 2020, 207: 118289
125. Alaba P A, Popoola S I, Abnisal F, Lee C S, Ohunakin O S, Adetiba E, Akanle M B, Abdul Patah M F, Atayero A A A, Wan Daud W M A. Thermal decomposition of rice husk: a comprehensive artificial intelligence predictive model. Journal of Thermal Analysis and Calorimetry, 2020, 140(4): 1811–1823
126. Zhu X, Li Y, Wang X. Machine learning prediction of biochar yield and carbon contents in biochar based on biomass characteristics and pyrolysis conditions. Bioresource Technology, 2019, 288: 121527
127. Li H, Xu Q, Xiao K, Yang J, Liang S, Hu J, Hou H, Liu B. Predicting the higher heating value of syngas pyrolyzed from

sewage sludge using an artificial neural network. Environmental Science and Pollution Research International, 2020, 27(1): 785–797

128. Whiteman J K, Gueguim Kana E B. Comparative assessment of the artificial neural network and response surface modelling efficiencies for biohydrogen production on sugar cane molasses. BioEnergy Research, 2014, 7(1): 295–305
129. Zhang Y, Ahmad M S, Shen B, Yuan P, Shah I A, Zhu Q, Ibrahim M, Bokhari A, Klemeš J J, Elkamel A. Co-pyrolysis of lychee and plastic waste as a source of bioenergy through kinetic study and thermodynamic analysis. Energy, 2022, 256: 124678
130. Gan D K W, Loy A C M, Chin B L F, Yusup S, Unrean P, Rianawati E, Acda M N. Kinetics and thermodynamic analysis in one-pot pyrolysis of rice hull using renewable calcium oxide based catalysts. Bioresource Technology, 2018, 265: 180–190
131. Fong M J B, Loy A C M, Chin B L F, Lam M K, Yusup S, Jawad Z A. Catalytic pyrolysis of Chlorella vulgaris: kinetic and thermodynamic analysis. Bioresource Technology, 2019, 289: 121689
132. Kumar Mishra R, Mohanty K. Co-pyrolysis of waste biomass and waste plastics (polystyrene and waste nitrile gloves) into renewable fuel and value-added chemicals. Carbon Resources Conversion, 2020, 3: 145–155
133. Abnisa F, Wan Daud W M A. A review on co-pyrolysis of biomass: an optional technique to obtain a high-grade pyrolysis oil. Energy Conversion and Management, 2014, 87: 71–85
134. Scheirs J. Feedstock recycling and pyrolysis of waste plastics. Manhattan: John Wiley & Sons Inc., 2006: 381–433
135. Gouws S M, Carrier M, Bunt J R, Neomagus H W J P. Co-pyrolysis of coal and raw/torrefied biomass: a review on chemistry, kinetics and implementation. Renewable & Sustainable Energy Reviews, 2021, 135: 110189
136. Lede J. Biomass fast pyrolysis reactors: a review of a few scientific challenges and of related recommended research topics. Oil & Gas Science and Technology, 2013, 68(5): 801–814
137. Venderbosch R, Prins W. Fast pyrolysis technology development. Biofuels, Bioproducts & Biorefining, 2010, 4(2): 178–208
138. Yousef S, Eimontas J, Stasiulaitiene I, Zakarauskas K, Striūgas N. Pyrolysis of all layers of surgical mask waste as a mixture and its life-cycle assessment. Sustainable Production and Consumption, 2022, 32: 519–531
139. Brassard P, Godbout S, Hamelin L. Framework for consequential life cycle assessment of pyrolysis biorefineries: a case study for the conversion of primary forestry residues. Renewable & Sustainable Energy Reviews, 2021, 138: 110549
140. Neha S, Prasanna Kumar Ramesh K, Remya N. Techno-economic analysis and life cycle assessment of microwave co-pyrolysis of food waste and low-density polyethylene. Sustainable Energy Technologies and Assessments, 2022, 52: 102356
141. Joshi V V, Swaminathan G, Prabhakaran S P S. Life cycle assessment of the co-combustion system of single-use plastic waste and lignite coal to promote circular economy. Journal of Cleaner Production, 2021, 329: 129579